

MINISTRY OF EDUCATION AND SCIENCE  
OF THE REPUBLIC OF KAZAKHSTAN

Kazakh National Research Technical University named after K. Satbayev

Institute of Geology and Oil and Gas Engineering named after K. Turysov

Department of Geophysics and Seismology

Ni Milana

Title: Methods for Integrating Aeromagnetic Survey Data with Geophysical and Geological  
Information to Enhance the Accuracy of Mineral Deposit Prediction»

**DIPLOMA WORK**

6B07201 – Oil and Ore Geophysics

Almaty 2025

MINISTRY OF EDUCATION AND SCIENCE  
OF THE REPUBLIC OF KAZAKHSTAN

Kazakh National Research Technical University named after K. Satbayev  
Institute of Geology and Oil and Gas Engineering named after K. Turysov  
Department of Geophysics and Seismology

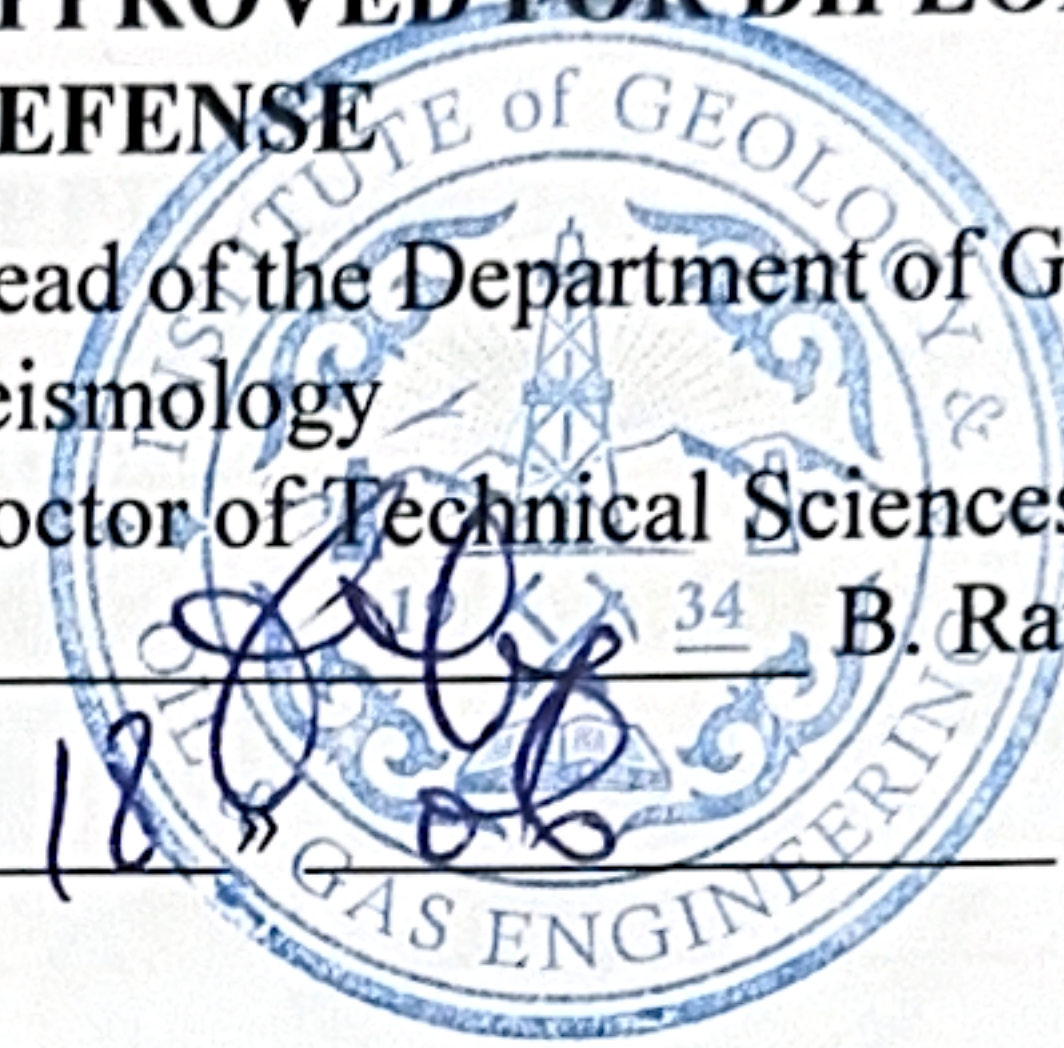
**APPROVED FOR DIPLOMA WORK  
DEFENSE**

Head of the Department of Geophysics and  
Seismology

Doctor of Technical Sciences, Professor

 B. Ratov

« 18 » 06 2025



**DIPLOMA WORK**

Title: «Methods for Integrating Aeromagnetic Survey Data with Geophysical and Geological Information to Enhance the Accuracy of Mineral Deposit Prediction»

6B07201 – Oil and Ore Geophysics

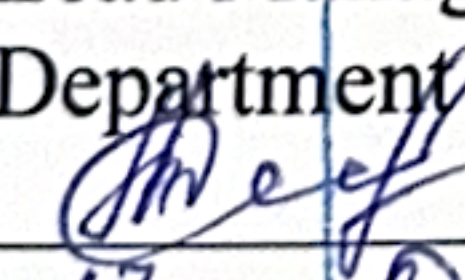
Prepared by

Ni Milana

Reviewer

Lead Manager of Geophysical

Department

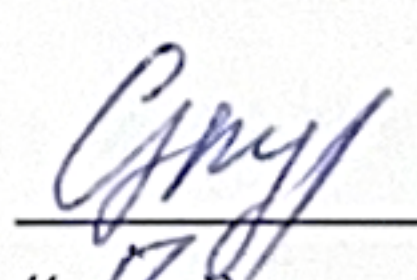
 D. Tukasbayeva

« 17 »



Project Supervisor

Associate Professor, Doctor Ph.D.

 R. Temirkhanova

« 17 » 06 , 2025

Almaty 2025

MINISTRY OF EDUCATION AND SCIENCE  
OF THE REPUBLIC OF KAZAKHSTAN

Kazakh National Research Technical University named after K. Satbayev  
Institute of Geology and Oil and Gas Engineering named after K. Turysov

Department of Geophysics and Seismology

6B07201 – Oil and Ore Geophysics

**APPROVED**

Head of the Department of Geophysics and  
Seismology

Doctor of Technical Sciences, Professor

B. Ratov

« 18 » 2025



**ASSIGNMENT**  
**for the Completion of the Diploma Work**

Student: Milana Ni

Title: «Methods for Integrating Aeromagnetic Survey Data with Geophysical and Geological Information to Enhance the Accuracy of Mineral Deposit Prediction»

Approved by the Order № 26-11/0 dated 29.01, 2025.

Deadline for submission of the completed work: "19" 06, 2025.

Initial data for the graduation project: were collected during the pre-graduation internship.

Brief summary of the graduation project:

a) *General information about the deposit (geological and geophysical characteristics of the deposit, geological and geophysical exploration status, tectonics, stratigraphy, intrusive formations, mineral resources);*

b) *Methodology of conducting geophysical surveys;*

c) *Methodology of processing geophysical data;*

d) *Geological interpretation.*

List of graphic material: 19 slides of presentation of works are presented.

Recommended basic literature: of 29 titles \_\_\_\_\_

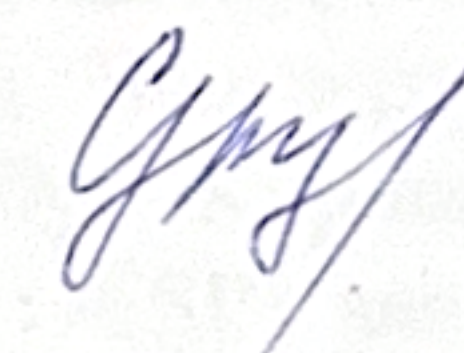
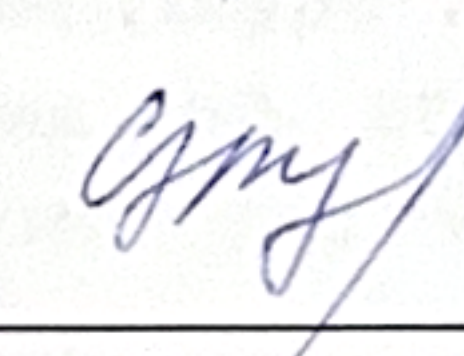
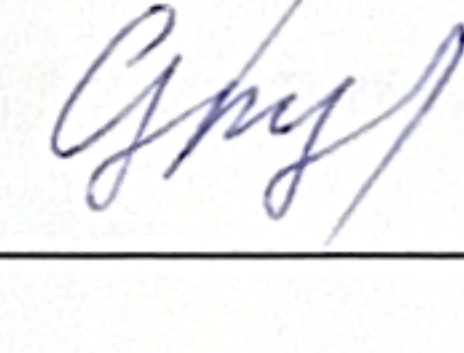
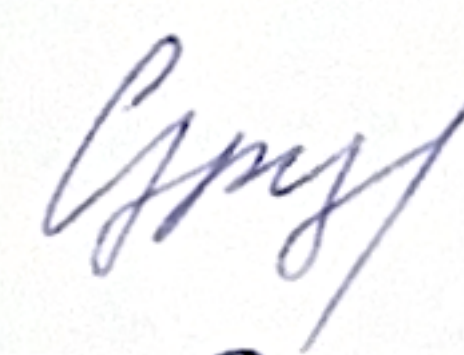
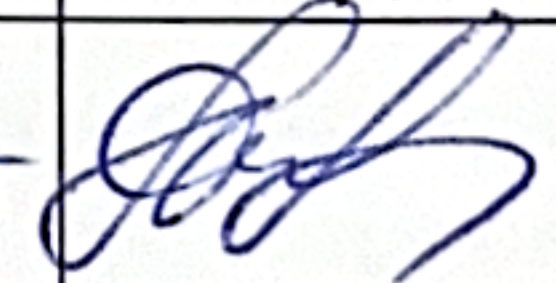
## SCHEDULE

or the Preparation of the Diploma Work

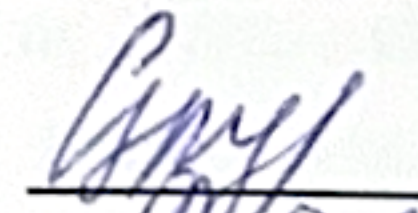
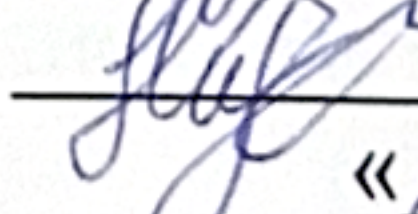
Titles of Sections and List of Topics to be Developed	Deadlines for Submission to the Scientific Supervisor	Note
Geological and geophysical characteristics of the Paterson survey area	26.03.2025	
Paleovalley-related uranium mineral systems	15.04.2025	
The TEMPEST™ AEM system	23.04.2025	
Paterson Orogen - gravity and aeromagnetic interpretation	5.05.2025	

### Signatures

of Advisors and Norm Control Officer on the Completed Diploma Work with an Indication of the Relevant Sections of the Work

Titles of Sections	Advisors, Full Name (Academic Degree, Title)	Date of signing	Signature
Geological and geophysical characteristics of the Paterson survey area	Associate Professor, Doctor Ph.D., R. Temirkhanova	10.06.2025r.	
Paleovalley-related uranium mineral systems	Associate Professor, Doctor Ph.D., R. Temirkhanova	12.06.2025r.	
The TEMPEST™ AEM system	Associate Professor, Doctor Ph.D., R. Temirkhanova	14.06.2025r.	
Paterson Orogen - gravity and aeromagnetic interpretation	Associate Professor, Doctor Ph.D., R. Temirkhanova	15.06.2025r.	
Standardizer	Master of Technical Sciences, Senior Lecturer, Z. Ablesenova	16.06.2025	

Project Supervisor  
Assignment accepted by the student  
Date

 R. Temirkhanova  
 Milana Ni  
«17» 06, 2025

## ANNOTATION

to the diploma work «Methods for Integrating Aeromagnetic Survey Data with Geophysical and Geological Information to Enhance the Accuracy of Mineral Deposit Prediction»

The paper presents data from the Paterson Airborne Electromagnetic Survey (Paterson AEM), conducted to obtain reliable information for the scientific analysis of the energy potential of the Paterson region in Western Australia. This was the first regional geophysical survey implemented as part of the Onshore Energy Security Program (OESP) led by Geoscience Australia. The survey was carried out in collaboration with Fugro Airborne Surveys Pty. Ltd. using the TEMPEST™ system, an advanced time-domain electromagnetic (TEM) surveying technology.

This study explores the feasibility of applying this electromagnetic survey method to mineral deposits in Kazakhstan

## АҢДАТПА

дипломдық жұмысқа «Аэромагниттік барлау деректерін геофизикалық және геологиялық деректермен интеграциялау әдістері кен орындарын болжау дәлдігін арттыру үшін»

Бұл жұмыста Батыс Аустралиядағы Патерсон өңірінің энергетикалық ресурстар әлеуетін ғылыми тұрғыдан талдау үшін және сенімді деректер алу мақсатында жүргізілген аэроэлектромагниттік зерттеулердің (Paterson AEM) нәтижелері ұсынылған. Бұл зерттеуді Австралия Геологиялық қызметі (Geoscience Australia) жүзеге асырған. Бұл Құрлықтық энергетикалық қауіпсіздік бағдарламасы (Onshore Energy Security Program, OESP) аясында жүргізілген алғашқы аймақтық геофизикалық зерттеу болып табылады. Зерттеуде *Fugro Airborne Surveys Pty. Ltd.* компаниясымен бірлесіп, TEMPEST™ жүйесі қолданылған, аталған time-domain electromagnetic, TEM әдісі өз кезегінде алдыңғы қатарлы технология болып табылады.

Осы жұмыста аталған электромагниттік зерттеу әдісін Қазақстан кен орындарында қолдану мүмкіндігі қарастырылған

## АННОТАЦИЯ

к дипломной работе «Методы интеграции данных аэромагниторазведки с геофизическими и геологическими данными для повышения точности прогнозирования месторождений»

В работе представлены данные аэроэлектромагнитных исследований района Патерсон (Paterson AEM), проведённых с целью получения достоверной информации для научного анализа энергетического потенциала региона Патерсон в Западной Австралии. Это было первое региональное геофизическое исследование, выполненное в рамках Программы энергетической безопасности на суше (Onshore Energy Security Program, OESP), реализуемой Геонауками Австралии (Geoscience Australia). Работы проводились совместно с компанией *Fugro Airborne Surveys Pty. Ltd.* с использованием системы TEMPEST™ — передовой технологии электромагнитной съёмки во временной области (time-domain electromagnetic, TEM).

В настоящей работе рассматривается возможность применения данного метода электромагнитных исследований на месторождениях Казахстана.

## CONTENTS

Introduction	7
1 General information	8
2 Geological and geophysical characteristics of the Paterson survey area	9
2.1 Paterson Orogen	10
2.2 The Rudall Complex	10
2.3 Yeneena Basin	12
2.4 Throssell Range Group	12
2.5 Isdell Formation	14
2.6 Lamil Group	14
2.7 Intrusions of the Yeneena Basin	16
2.8 The Miles and Paterson orogenies	16
3 Paleovalley-related uranium mineral systems	17
4 The TEMPEST™ AEM system	20
5 Paterson Orogen - gravity and aeromagnetic interpretation	28
5.1 Gravity Characteristics	28
5.2 Aeromagnetic Characteristics	30
5.3 Canning Basin	33
5.4 Kintyre deposit	35
6 Comparative analysis of Australia and Kazakhstan	38
Conclusion	40
References	42

## INTRODUCTION

Title of the Thesis:

Methods for Integrating Aeromagnetic Survey Data with Geophysical and Geological Information to Enhance the Accuracy of Mineral Deposit Prediction

Relevance of the Research:

With the increasing demand for discovering new mineral deposits and improving the efficiency of geological exploration, the integration of various information sources becomes critically important. Aeromagnetic surveys provide extensive coverage and high sensitivity to geological inhomogeneities. However, to maximize their predictive value, these surveys must be complemented by other methods. An integrative approach enables more precise interpretation of geophysical anomalies, reduces prediction uncertainty, and increases the reliability of identifying promising areas. This study aims to adapt and develop such approaches for Kazakhstan's conditions, which holds significant practical relevance for the country's mineral resources sector.

Research Objective:

To study effective methods for integrating aeromagnetic survey data with geophysical and geological information to enhance the accuracy of mineral deposit predictions.

Research Tasks:

- 1) Examine modern approaches to integrating aerogeophysical, geophysical, and geological data.
- 2) Investigate examples of successful application of integrative methods in international practice (using the Paterson region in Australia as a case study).
- 3) Assess the applicability of these methods to the geological conditions of Kazakhstan's mineral deposits.

Research Object:

Geophysical fields and geological structures identified through aeromagnetic surveys, combined with data from other geophysical and geological methods.

# 1 General information

In recent years, geophysical exploration methods have significantly enhanced the efficiency of mineral resource exploration. One such method is airborne electromagnetic (AEM) surveying, which allows for detailed mapping of subsurface geological structures associated with valuable energy resources.

The Paterson AEM survey primarily aimed to map subsurface geological structures that could host uranium deposits associated with unconformities, sandstones, or paleovalleys. These deposit types represent a significant portion of the world's known uranium resources, accounting for over 25% of the total. Paleovalley-related uranium deposits are particularly noteworthy, as they provide medium-grade uranium resources at relatively low costs. Such deposits are found in various regions worldwide, including the Central Asian Uranium Province (CAUP), Australia, the United States, Niger, Gabon, and South Africa.

The main goal of The Paterson Airborne Electromagnetic Survey (Paterson AEM) was to reduce exploration risks, attract investments, and enhance the prospectivity of the region for energy resources, particularly uranium. The survey area covered parts of several 1:250,000 map sheets, including ANKETELL, BALFOUR DOWNS, GUNANYA, NULLAGINE, PATERSON RANGE, RUDALL, RUNTON, TABLETOP, and YARRIE.

The objective of this study is to conduct a detailed analysis of the Paterson AEM data, interpret the results using modern geophysical methods, and assess the resource potential of the region for various minerals, including uranium. Integrating global data on paleovalley-related uranium systems with lithological-geochemical mapping in Kazakhstan provides a broader context for understanding and identifying prospective targets on both regional and local scales.

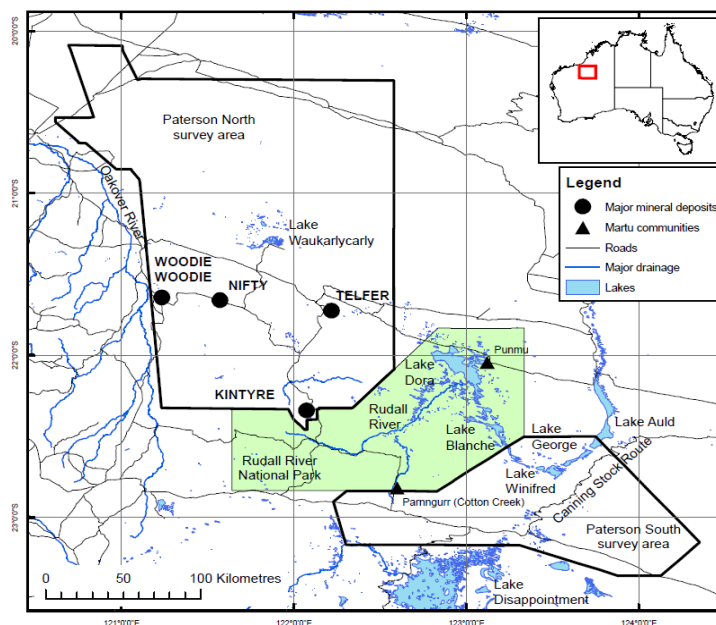


Figure 1.1 -Survey location showing the principal mineral deposits, settlements, access roads and major drainage systems

## **2 Geological and geophysical characteristics of the Paterson survey area**

The Paterson survey area encompasses four main tectonic units: the Pilbara Craton to the west, the Paterson Orogen located centrally, the Officer Basin sediments to the south, and the Canning Basin sediments to the north and east. Among these, the Paterson Orogen is of particular interest, as it forms the primary focus of this study due to its significance in hosting uranium-bearing formations, alongside its central geological position in the region.

The Paterson Orogen is recognized as the most uranium-enriched tectonic unit in the area, hosting major deposits such as the Kintyre and Manyingee uranium deposits. The Kintyre deposit is one of the largest in the region and is associated with granitic and gneissic complexes in the northeastern part of the orogen. In contrast, the Manyingee deposit features uranium mineralization within water-saturated sandstone beds, a characteristic typical of sedimentary-hosted uranium deposits. These deposits highlight the importance of the Paterson Orogen as a key area of interest for both geological and resource studies.

The Officer Basin, located to the south of the Paterson Orogen, also contains uranium occurrences, primarily associated with sedimentary rocks. One notable example is the Mount Gee deposit, where uranium mineralization is linked to zones of geothermal alteration within the basin's sedimentary sequences.

Similarly, the Canning Basin to the north and east contains uranium deposits, though on a lesser scale compared to the Paterson Orogen. Noteworthy among these is the Yeelirrie deposit, which is associated with carbonate-rich sediments and demonstrates the potential for uranium mineralization within the basin's depositional environment.

In contrast, the Pilbara Craton, located to the west, has limited uranium occurrences. While there are minor uranium manifestations associated with pegmatites and hydrothermal processes in the ancient granitic and metamorphic rocks, the craton does not host significant deposits comparable to those in the Paterson Orogen or adjacent basins.

This study will primarily examine the geological and geophysical characteristics of the Paterson Orogen, emphasizing its role as a host for major uranium deposits. Additionally, the interrelations with adjacent tectonic units, particularly the sedimentary basins, will be considered to provide a comprehensive understanding of the uranium distribution in the region.

Airborne electromagnetic acquisition by Geoscience Australia and five infill companies was undertaken in two areas north and south of the Rudall River National Park. These areas are referred to below as 'Paterson North' and 'Paterson South'. In the following description of the Precambrian geology, reference will be made to regional gravity and aeromagnetic data and their interpretation.

The whole of the area is covered by an 11 km spaced regional gravity grid acquired by the Bureau of Mineral Resources, predecessor of Geoscience Australia. Most of Paterson North has also been covered by a 2.5 km spaced gravity survey acquired in 2005 by the Geological Survey of Western Australia. Some additional

complementary infill gravity data was acquired from Barrick Gold Corporation. All of Paterson North and much of Paterson South are covered with 400 m linespaced aeromagnetic data acquired at a ground clearance of 60-80 m and ca. 15 m along-line sampling. The southern part of Paterson South on GUNANYA and RUNTON is covered with older regional 1500 m line-spaced aeromagnetic data acquired at a ground clearance of 150 m and ca. 60 m along-line sampling.

The sample- and line-spacing of these surveys places relative constraints on their ability to resolve near-surface geological features. Other factors that influence resolution of geological features include the distribution and variability of rock properties (density, susceptibility and remanence) and the drop in anomaly amplitude with distance (depth) to the source: gravity anomalies decrease with the square of the distance; and, aeromagnetic anomalies decrease with the cube of the distance. Thus, in combination with respective station spacings, gravity data often show deeper, and aeromagnetic data shallower, information on lithology and structural patterns.

## **2.1 Paterson Orogen**

The Paterson Orogen consists of metamorphosed Paleoproterozoic to Neoproterozoic sediments and igneous rocks which were variably deformed during the Miles (ca. 1070 > 650 Ma; Bagas, 2000) and Paterson (ca. 650-550 Ma; Bagas et al., 1995; Bagas et al., 1999) orogenies. The Rudall Complex forms the basement of the Paterson Orogen and underwent amphibolite to granulite facies metamorphism during the Yapungku Orogeny (ca. 2015-1760 Ma; Bagas et al., 2000). The Complex consists of supracrustal and igneous rocks of Paleoproterozoic to Mesoproterozoic age. Unconformably overlying these rocks are greenschist facies Neoproterozoic sediments of the Yeneena Basin. These sediments were folded and faulted during the Miles Orogeny and were subsequently intruded by granite. Faulting during the Paterson Orogeny further deformed the Rudall Complex and the south-western margin of the Yeneena Basin. The Rudall Complex is host to the Kintyre uranium deposit, whereas sediments of the Yeneena Basin host the Telfer (gold-copper), Nifty (copper) and O'Callaghans (tungsten-base metal skarn) deposits. Numerous other small mineral occurrences occur throughout the Paterson Orogen.

## **2.2 The Rudall Complex (Paleo- to Mesoproterozoic)**

The Rudall Complex crops out from central southern Paterson North, through the Rudall River National Park, southeast into western and central Paterson South. The complex was previously subdivided into three terranes with distinct lithological make up: the Talbot; Connaughton; and, Tabletop Terranes. While the Talbot and Connaughton Terranes are inferred to have undergone similar geological evolution, the

Tabletop Terrane is considered to be significantly different, particularly in the timing of voluminous felsic magmatism.

The Talbot Terrane is composed largely of orthogneiss and metamorphosed siliciclastic sedimentary rocks. While the Terrane has been significantly disrupted by faulting and thrusting, sufficient detail of lithostratigraphic relationships have been preserved in the metasedimentary rocks to enable development of a stratigraphic succession.

Talbot Terrane metasedimentary stratigraphy, after Hickman and Bagas (1998):

Top

1) Poynton Formation. Thickness ca. 1 km. Quartzite, meta-greywacke, quartz-muscovite schist, minor pelitic schist and banded iron formation.

2) Butler Creek Formation. Thickness >1 km. Pelitic schist, paragneiss and local banded iron formation.

3) Yandagooge Formation. Thickness < 1500 m. Quartz-muscovite schist, meta-pelitic rocks, banded iron formation, chert, graphitic schist and biotite schist.

4) Fingoon Quartzite. Thickness > 1500 m. Quartzite and micaceous quartzite.

5) Larry Formation. Unknown thickness. Quartz-feldspar-mica paragneiss and quartz mica schist.

Bottom

Widespread orthogneiss was derived mostly from monzogranite to granodiorite compositions and rarely tonalite. Emplacement ages for protoliths of orthogneiss of between 2015 and 1765 Ma are inferred to provide minimum depositional ages of paragneiss in the terrane. While some paragneiss must be older than 2015 Ma, the Fingoon Quartzite is younger than 1790 Ma, the age of contained detrital zircons. The stratigraphically or structurally overlying Yandagooge and Butler Creek formations were intruded by, and must be older than, granite ranging in age from 1790 to 1756 Ma. A greater abundance of intrusive ages for the granitic protolith of orthogneiss, in the range of 1790 to 1765 Ma, is considered to be coincident with the second phase, including D2 deformation and high pressure metamorphism, of the Yapungku Orogeny. Orthogneiss, Fingoon Quartzite and Yandagooge Formation outcrop in southern Paterson North and western Paterson South.

The Connaughton Terrane is located to the east and southeast of the Talbot Terrane and is composed of approximately 50% mafic and ultramafic rocks with successively lesser quantities of gneiss and schist of unknown protolith, orthogneiss, metasedimentary rocks, granite and pegmatite. Stratigraphic relationships are poorly defined due to structural dismemberment and lack of well defined primary layering. Rocks of the Connaughton Terrane underwent high pressure amphibolite to granulite metamorphism during the latter part of the Yapungku Orogeny and were intruded by similarly-aged protoliths to the orthogneiss during that event.

The Tabletop Terrane abuts the Connaughton Terrane to the northeast across the northwest-trending Camel-Tabletop Fault. Granite and pegmatite account for approximately 70% of the terrane with lesser abundances of mafic, ultramafic and metasedimentary rocks. Tonalite is the dominant granitic rock type and is largely undeformed except adjacent to the Camel-Tabletop Fault. The terrane has undergone

low pressure metamorphism to lower amphibolite grade and was extensively intruded by granite between 1590 and 1310 Ma. Augen gneiss, abundant in the adjacent Talbot and Connaughton terranes, is absent from the Tabletop Terrane. The contrast in rock type abundances, pressure of metamorphism and lack of 1590-1310 Ma granite in the adjacent terranes is thought to indicate that the Tabletop Terrane developed separately and was subsequently tectonically emplaced.

The Rudall Complex is overlain unconformably to the north by sediments of the Yeneena Basin and to the southeast by sediments of the Tarcunyah Group. Permian glacial sediments of the Paterson Formation were subsequently deposited in palaeovalleys that cut across the region of outcrop of the complex. The whole is overtopped by Mesozoic sediments of the Canning Basin.

### **2.3 Yeneena Basin (Neoproterozoic)**

The Yeneena Basin crops out largely to the north of exposures of the Rudall Complex, underlies much of the Paterson North survey area and consists of the Throssell Range Group and the Lamil Group. Precise depositional ages of the groups are not known and contacts between the groups are not observed in outcrop. The Throssell Range and Lamil groups are younger than contained ca. 950 Ma detrital zircons and the Lamil Group is older than the ca 650-630 sensitive high-resolution ion microprobe (SHRIMP) uranium-lead (U-Pb) isotopic age of the Mount Crofton Granite Suite which intrudes it. On BROADHURST, carbonate-rich Isdell Formation lies between the two groups, but again no stratigraphic relationships have been determined as contacts with the Throssell Range Group to the south are obscured by Cenozoic sediment and the Isdell Formation is in tectonic contact with the Lamil Group across the Parallel Range Fault to the north-northeast. The Isdell Formation is older than monzonite and gabbro intrusives dated at ca. 830 Ma.

### **2.4 Throssell Range Group (thickness > 7km)**

In Paterson North, the Coolbro Sandstone is the lowermost unit of the Throssell Range Group and unconformably overlies the Rudall Complex. The formation is up to 4 km thick and is largely composed of fine- to coarse-grained sandstone. The sandstone tends to have finer grain sizes in the upper parts where siltstone lenses are interbedded. These finer grained sandstone and siltstone units mark a transition to the overlying Broadhurst Formation. Deposition occurred in a fluvio-deltaic environment with sediment derived from the adjacent Rudall Complex. Hickman and Bagas (1998) suggested the regional depositional setting was that of a strike-slip basin with initiation associated with the onset of the Miles Orogeny. The Broadhurst Formation conformably overlies the Coolbro Sandstone and consists of upper and lower sections, dominantly composed of carbonaceous shale/pelitic schist, with an intervening interval

of argillaceous turbiditic greywacke and sandstone. The shale-dominated sections include beds with up to 10% pyrite and pyrrhotite, the latter giving rise to aeromagnetic heights. Beds of limestone and dolomite, generally less than 100 m thickness, are particularly associated with the carbonaceous shale components. The Formation is estimated to be 2-3 km thick and is inferred to have been deposited in a fault-controlled, sediment-starved basin under euxinic conditions. A generalised stratigraphy for the Throssell Range Group is given in Figure 2.1.

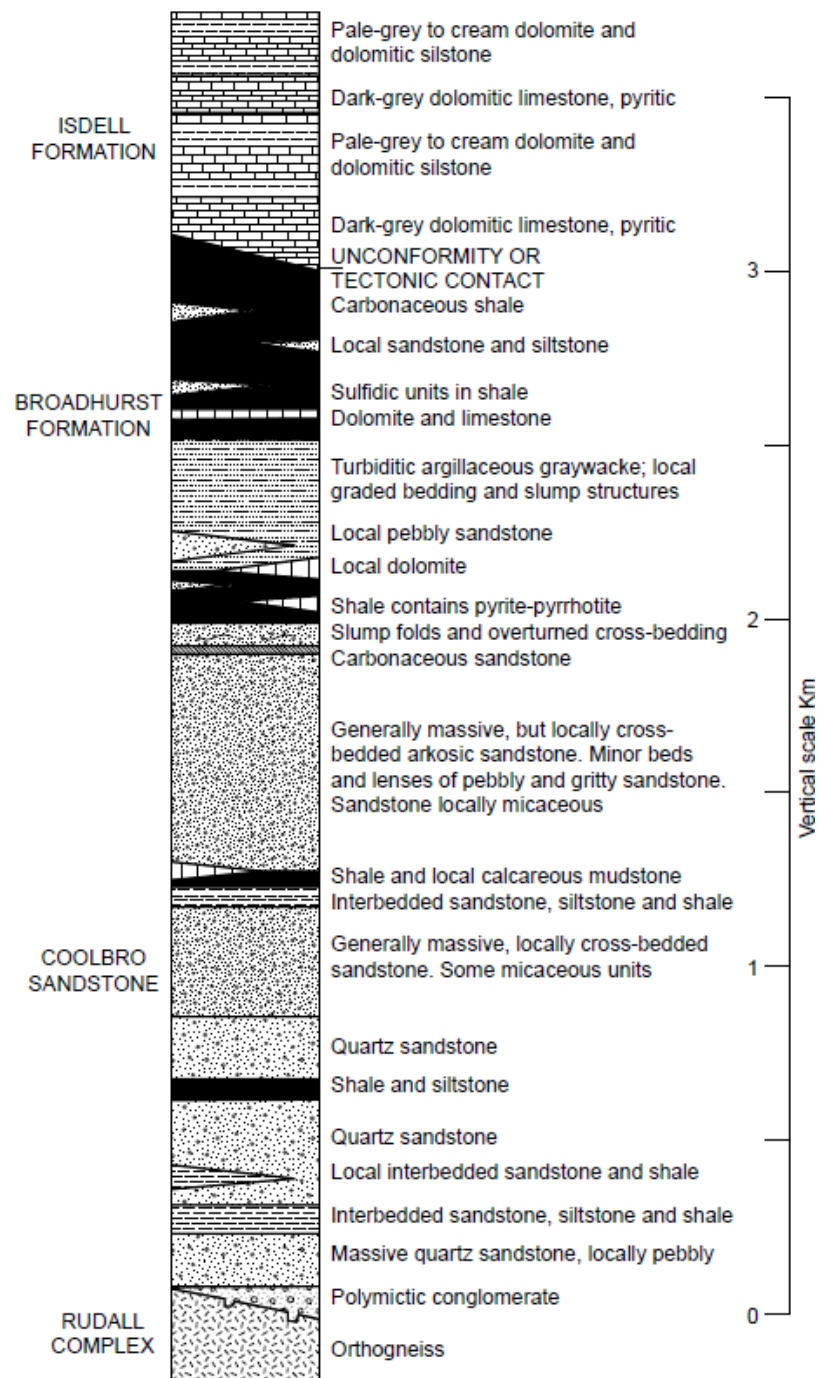


Figure 2.1 - Generalised stratigraphy of the Throssell Range Group and Isdell Formation, redrawn from Hickman and Clarke (1994)

Throssell Range Group stratigraphy, Paterson North, after Hickman and Clarke (1994):

Top

1) Broadhurst Formation. Thickness 2 to 3 km. Carbonaceous shale (pyrite and pyrrhotite to 10%) with minor carbonate lenses, argillaceous turbiditic greywacke and sandstone.

2) Coolbro Sandstone. Thickness, 3 to 4 km. Fine- to coarse-grained sandstone with local basal conglomerate.

Bottom

In Paterson South and to the immediate north, polymictic conglomerate and arkosic sandstone of the Taliwanya Formation lies unconformably on the Rudall Complex. The Formation is up to 170 m thick and is overlain by the Pungkuli Formation, which is composed of up to 900 m of black shale, sandstone and pyritic shale. These two formations have also been assigned to the Throssell Range Group and may be correlatives of Coolbro Sandstone and overlying Broadhurst Formation outcropping further north.

## **2.5 Isdell Formation (Thickness > 1km)**

The Isdell Formation outcrops poorly in a region between better exposed Broadhurst Formation to the south and Lamil Group to the north. The Formation is estimated to be over 1 km thick and is composed of dolomitic limestone and limestone intercalated with calcareous siltstone and shale. Stratigraphic relationships with the adjacent groups have not been determined due to Cenozoic sediment cover of the contact with Broadhurst Formation and faulted contacts with the Lamil Group. Hickman and Clarke (1994) noted a discontinuity in aeromagnetic data corresponding to the position of the Broadhurst-Isdell formation boundary which they attributed to either an unconformity or a tectonic contact.

Minimum depositional age constraints for the Isdell Formation are provided by monzonite and gabbro intrusives which yielded emplacement ages of ca. 830 Ma. An unpublished pooled lead-lead isotopic (Pb-Pb) age of 858 +/- 29 Ma from thinly bedded limestone, calcareous siltstone and argillaceous siltstone samples is thought to date diagenesis of the Formation.

## **2.6 Lamil Group (Thickness 4-5 km)**

The Lamil Group is a sandstone-shale-carbonate succession which Turner (1982) suggested was deposited in an intracratonic setting at a continental margin or in a failed rift. The lowermost unit, the Malu Formation, is in the order of 1-2 km thick and consists of shale, sandstone and siltstone with thin carbonate units present towards the top. The Puntapunta Formation conformably overlies the Malu Formation and consists of dolomitic siltstone, rare limestone, dolomitic sandstone, chert and shale.

The Puntapunta Formation is up to 1.5 km thick and was deposited in a carbonate-dominated shelf environment. The Wilki Formation is inferred to conformably overlie the Puntapunta Formation, however, contacts are not exposed. The Wilki Formation is approximately 1.4 km thick and is composed of a lower section of graphitic shale, siltstone and fine grained silty sandstone overlain by fine- to medium-grained sandstone with interbedded silty sandstone. A shallow marine environment was proposed by Turner (1982) for deposition of the Wilki Formation.

In recent mapping of Yeneena Basin sediments on PATERSON, several outcrops have not been assigned to named formations. For instance, massive sandstone with minor interbedded dolomitised shale in the northeast, although having similar descriptions, outcrop pattern and aeromagnetic characteristics to the Wilki Formation, is separated by a major concealed structural break from the Wilki Formation and therefore could not be correlated with certainty. Also, dolomite with interbedded siltstone to the south of the Parallel Range Fault, which was previously correlated with the Isdell Formation by Chin et al. (1982), remains unassigned in the most recent mapping. The 10 km distance between these exposures and outcropping Isdell Formation to the south, lithological similarity with Puntapunta Formation and lack of known stratigraphic context due to the faulted contact with Malu Formation to its north were the reasons given for lack of assignment.

Lamil Group stratigraphy, after Bagas (2000):

Top

1) Wilki Formation. Thickness 1.4 km. Graphitic shale, siltstone, fine grained silty sandstone and fine- to medium-grained sandstone.

2) Puntapunta Formation. Thickness 1.5 km. Dolomitic siltstone and sandstone, chert and shale.

3) Malu Formation. Thickness 1-2 km. Shale, sandstone and siltstone with thin carbonate units in the upper part.

Bottom

The Lamil Group extends under gently deepening cover to the north of outcropping areas in a structural high known as the Anketell Shelf. In this area the Group is unconformably overlain by Mesozoic sediments immediately and Paleozoic and Mesozoic sediments farther north. Both to the west and east cover increases more rapidly and includes Ordovician to Permian sediments in the Waukarlyarly Embayment to the west and Canning Basin to the east. Because of the inferred prospectivity of the Lamil Group, which hosts the Telfer gold-copper deposit, much exploration drilling has been undertaken in the vicinity of the Shelf. However, nearly 50% of this drilling failed to reach the prospective rocks underneath the cover materials. A lack of knowledge of the distribution of cover thickness is a likely factor in the relatively ineffective drilling.

## **2.7 Intrusions of the Yeneena Basin**

The Lamil Group has been intruded extensively by generally undeformed, highly fractionated granites with compositions ranging from monzogranite to syenogranite. The Mount Crofton and associated granite suites have yielded inferred intrusive ages in the range of 650 to 630 Ma. Surrounding contact metamorphic aureoles of varying widths of up to 2 km have been developed and reached the pyroxene hornfels facies of metamorphism.

The Paterson Orogen has also been intruded by numerous mafic dykes and sills. Dolerite on BROADHURST has yielded rubidium-strontium (Rb-Sr) isotopic ages of 700 to 750 Ma, however, some dykes intruding the Rudall Complex are inferred to postdate all deformation.

## **2.8 The Miles and Paterson orogenies**

The Yeneena Basin has been deformed by two main orogenic events, the Miles and Paterson orogenies, but the ages of these orogenies are not well constrained. The Miles Orogeny is younger than the ca. 950 Ma detrital zircons in both the Throssell Range and Lamil groups, and older than the 650-630 Ma intrusive age of the Mount Crofton Granite which intrudes the Lamil Group and imposed structure. The Orogeny (D3-4) produced large scale northwest-trending faults and widespread, similarly aligned folds in the Throssell Range and Lamil groups. Local thrusts and recumbent folds were developed in the Throssell Range Group. Southwest-directed shortening also produced conjugate north-northeast- and east-southeast-trending faults with dextral and sinistral movements respectively. Widespread soft sediment deformation of the Lamil Group is thought to indicate the orogeny occurred early in the history of the Group. Both the Throssell Range and Lamil groups underwent lower or sub-greenschist metamorphism during this event while the Rudall Complex underwent extensive retrogressive metamorphism to greenschist facies.

The Paterson Orogeny occurred after the Miles Orogeny, but more detailed constraints are not well documented from within the Paterson Orogen. Howard et al. (2005) inferred the timing of the Orogeny was closely linked with intrusion of granite and thermal metamorphism in the Telfer area and therefore occurred about 650-630 Ma. However, Williams (1992) and Williams and Tyler (1991) state that the Orogeny occurred after deposition of the ca. 610 Ma Boondawari Formation of the northwest Officer Basin. The Orogeny has been correlated with the Petermann Orogen of central Australia at about 550 Ma but this speculative view requires more factual constraints to firm a tectonic connection.

Deformation resulting from south-southwest directed shortening produced folds with east to east-southeast fold axes and north-northwest and east-southeast, near-vertical strike-slip faults with dextral and sinistral movements respectively. The Camel-Tabletop Fault is inferred to have been reactivated during the Orogeny with evidence

for both vertical and strike-slip movements. There is no evidence in the regional geophysical data to suggest that the Lamil Group was subsequently deformed around the Mount Crofton and O'Callaghans Suite granites after intrusion, or, that there was any significant disruption of the granites by reactivated movement on northwesttrending faults. Thus, if the Paterson Orogeny occurred after the 650-630 Ma, deformation of the Lamil Group was relatively minor. Perhaps the main effects of the Orogeny were constrained between the Vines Fault in the west, the western Waukarlycarly-Camel-Tabletop faults to the east and the Southwest Thrust–McKay Fault system to the southwest and south respectively.

### **3 Paleovalley-related uranium mineral systems**

Paleovalley-related uranium deposits are unique geological features with significant economic potential and promising development prospects. Research into the geology of paleovalley uranium systems in Australia and Kazakhstan reveals both common characteristics and specific features, which in turn help refine strategies for mineral exploration.

These deposits form through complex processes of sedimentation, uranium migration, and concentration within sedimentary deposits filling ancient valleys. Paleovalleys incise crystalline basement or older sedimentary rocks, and their formation is linked to the circulation of oxidized or reduced groundwater, which facilitates uranium accumulation. Geological settings, age, sedimentary conditions, and hydrogeological characteristics of paleovalleys significantly influence uranium mineralization processes.

This study focuses on key characteristics of such deposits, including uranium sources, geochemical parameters, aquifer properties, and mechanisms of uranium remobilization and concentration. These aspects enable the creation of uranium mineralization models applicable for assessing regional prospectivity and setting exploration goals.

#### **Paleovalley-Related Uranium Deposits in Australia and Kazakhstan:**

##### **Australia**

In Australia, uranium deposits within the Paterson Province predominantly formed during the late Proterozoic and early Paleozoic. Their formation is closely tied to paleovalleys—ancient river systems that served as channels for oxidizing waters. These waters transported uranium, depositing it in sandstone formations. The arid climate of the region played a crucial role in forming oxidized zones where uranium minerals precipitated. One notable example is the Kintyre deposit, where uranium minerals are associated with calcite formations resulting from minimal leaching conditions.

##### **Kazakhstan**

In Kazakhstan, the Chu-Sarysu Basin is a key region for uranium mineralization. Deposits here formed during the Cretaceous and Paleogene periods of the Mesozoic-Cenozoic era. Intense tectonic activity during this time facilitated the formation of

sedimentary platform complexes, creating favorable conditions for uranium leaching and migration via groundwater. This resulted in stratiform-infiltration uranium deposits in sandstone horizons, characteristic of Southern Kazakhstan's deposits.

Despite differences in geological age and tectonic processes, Australia and Kazakhstan share common features in uranium deposit formation. In both cases, paleovalleys played a crucial role in transporting and depositing uranium in oxidized zones. The arid climate further contributed to uranium concentration in sedimentary complexes, underscoring the universal importance of climatic and hydrogeological factors in uranium system formation.

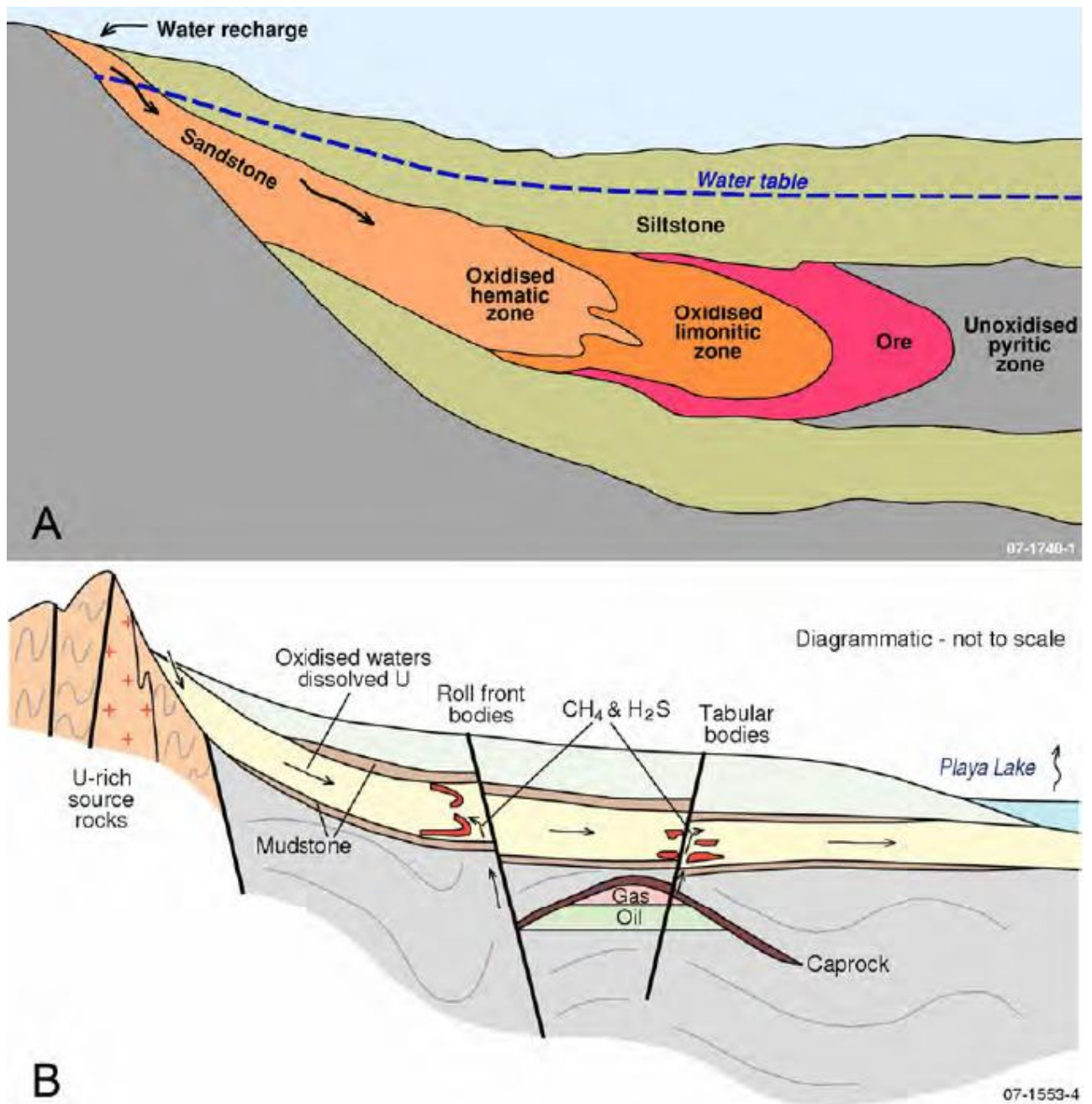


Figure 3.1 - Conceptual models of sandstone-hosted uranium mineral systems, A. single fluid model; B. two-fluid model

Sandstone-hosted uranium mineral systems are classified into two main types: those in confined aquifers (also known as roll-front and tabular types) and those in palaeochannels (also known as basal channel type). Both types of deposits are generally restricted to sediments deposited in continental fluvial or marginal marine (mixed fluvial-marine) environments.

Sandstone-hosted uranium deposits within confined aquifers form where uranium-bearing oxidized groundwater moving through sandstone aquifers reacts with reducing materials. In such systems, the formation of ore bodies is associated with the precipitation of uranium from solution. In a single-fluid situation, uranium carried by oxidized groundwater is reduced by in-situ reductants such as organic matter or other chemically active compounds within the sandstone. Groundwater flow tends to be faster in the central part of the aquifer than along contacts with less permeable units, such as mudstone, which leads to the formation of roll-front ore bodies characterized by their distinct shape and location.

In a two-fluid situation, uranium reduction occurs due to hydrocarbons and/or hydrogen sulfide released from underlying oil or gas fields. This process promotes uranium precipitation in ore bodies of various scales. Both roll-front and tabular ore bodies can form in such conditions. The location of ore zones and the size of mineral deposits depend on the quantity and reactivity of the reductants, making this parameter key to deposit prediction.

Uranium deposits in palaeochannels form through processes similar to roll-front and tabular types but are closely linked to the evolution of palaeodrainage systems in the region. These deposits may be associated with ancient river channels or other elements of the fluvial system, which determines their complex geometry and variability. The development of such systems, combined with geochemical conditions, creates favorable settings for uranium accumulation.

Studying the geological processes underlying the formation of sandstone-hosted uranium deposits is crucial for more accurate exploration methods and improving the efficiency of discovering new resources. The application of modern technologies, such as airborne geophysical methods and three-dimensional modeling, significantly enhances the understanding of the formation patterns of these deposits. Considering the specifics of geological and hydrogeological processes allows the development of optimized exploration strategies, which is particularly important for the exploration and development of sandstone-hosted uranium deposits.

## 4 The TEMPEST™ AEM system

The survey area is located in the southwestern part of the Great Sandy Desert and includes the Paterson Orogen, Throssell and Gregory Ranges, Lake Waukarlycarly, and parts of the Rudall Complex and Percival Lakes system (Figure 5.1). Despite its geological diversity, the region presents significant logistical challenges, including limited road access and a small number of airstrips.

To enhance survey efficiency, flight lines were oriented perpendicular to the anticipated geological structures: east-west in the northern part of the area and northeast-southwest in the southern part. The spacing between lines varied from 6 km for regional coverage to 200 m for detailed examination in areas of interest.

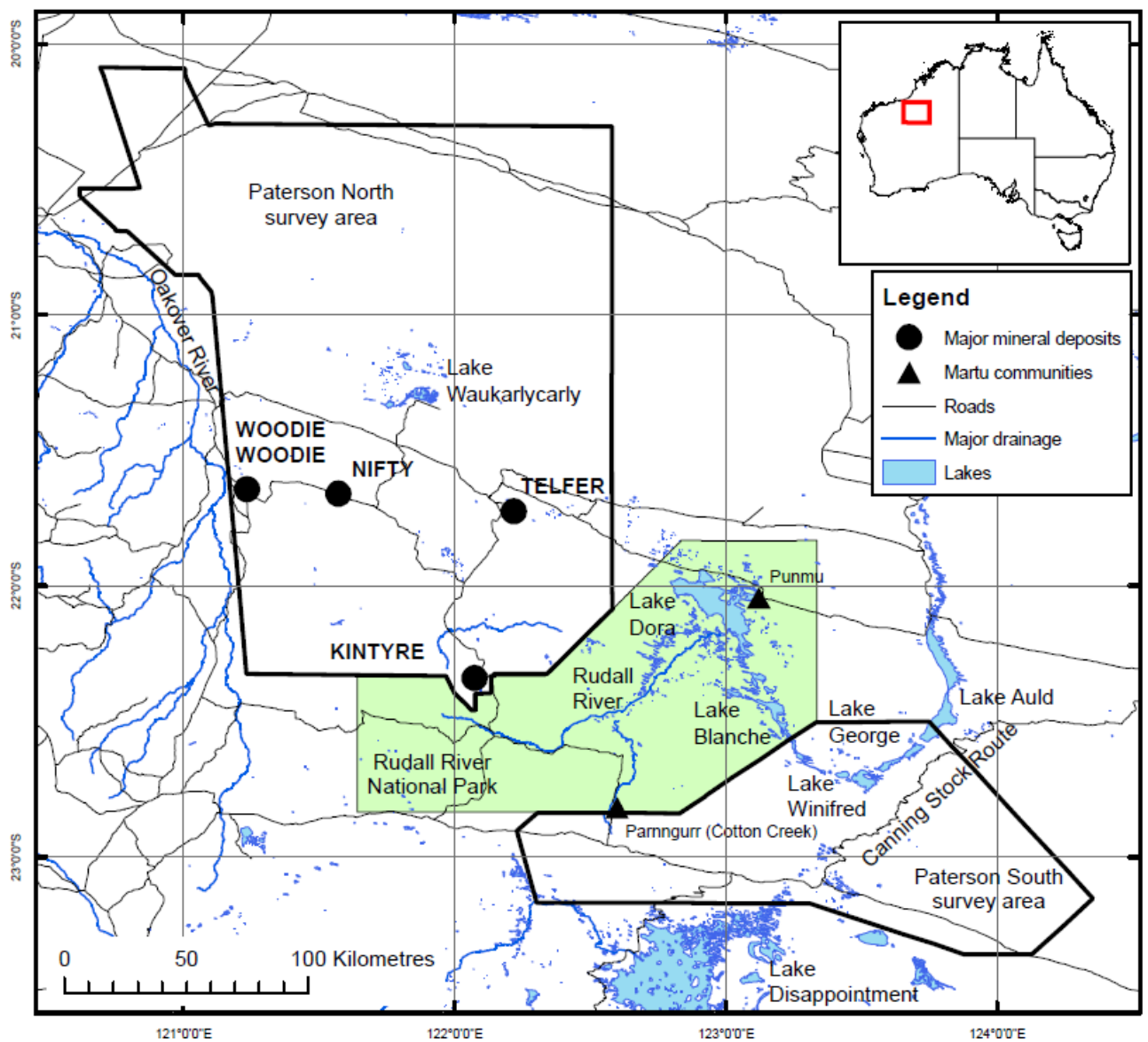


Figure 5.1 - Survey location showing the principal mineral deposits, settlements, access roads and major drainage systems

Airborne Electromagnetic (AEM) surveys are a widely utilized geophysical technique for mapping the electrical conductivity of subsurface materials across extensive areas. This method leverages natural variations in conductivity, which result from differences in rock and pore fluid properties. Electrically conductive materials, such as graphite, clays, sulfide minerals, or saline groundwater, exhibit higher conductivity than non-conductive assemblages or fresh groundwater, making AEM a valuable tool in resource exploration and environmental studies.

The principle of operation of AEM surveys involves an airborne platform, typically an aircraft or helicopter, equipped with a transmitter loop and receiver system. The transmitter loop generates a time-varying electromagnetic field that penetrates the subsurface, inducing secondary (eddy) currents in conductive materials. These currents create their own electromagnetic fields, which are measured by receiver coils towed beneath or behind the aircraft. The intensity and decay of the measured electromagnetic signals depend on the conductivity of the subsurface materials, enabling the estimation of their properties. The depth of investigation varies with system design and the conductivity contrast of the materials, reaching depths of several hundred meters. Shallow, highly conductive features are generally more readily detected, but AEM systems can also resolve deeper targets under suitable conditions.

AEM systems collect data at regular intervals along survey flight lines, with each sample representing the observed electromagnetic response from a specific point. The data include measurements of primary and secondary electromagnetic fields, along with auxiliary information such as flight altitude, terrain clearance, ground elevation, and noise levels caused by external sources like power lines or lightning. The raw data undergo extensive processing to remove noise and correct for system geometry. Advanced algorithms, such as forward modeling and inversion, are applied to transform the electromagnetic responses into conductivity-depth sections. These models depict the lateral and vertical variations in conductivity, providing insights into subsurface structures.

Geoscience Australia employs the GA-LEI inversion algorithm for many AEM datasets, producing detailed conductivity-depth profiles. This approach incorporates probabilistic Bayesian inversion techniques to quantify uncertainties in the derived models, enhancing the reliability of the interpretations. These interpretations enable the detection of geological units such as clay-rich layers, graphite-bearing zones, or sulfide-rich mineralization, and the definition of aquifer boundaries or structural features like unconformities and faults that influence resource distribution. Integrating AEM data with other geophysical datasets, such as magnetics and gravity, and borehole measurements improves the accuracy of geological models. The results are often represented as 3D conductivity models, gridded depth slices, or multi-plot data visualizations.

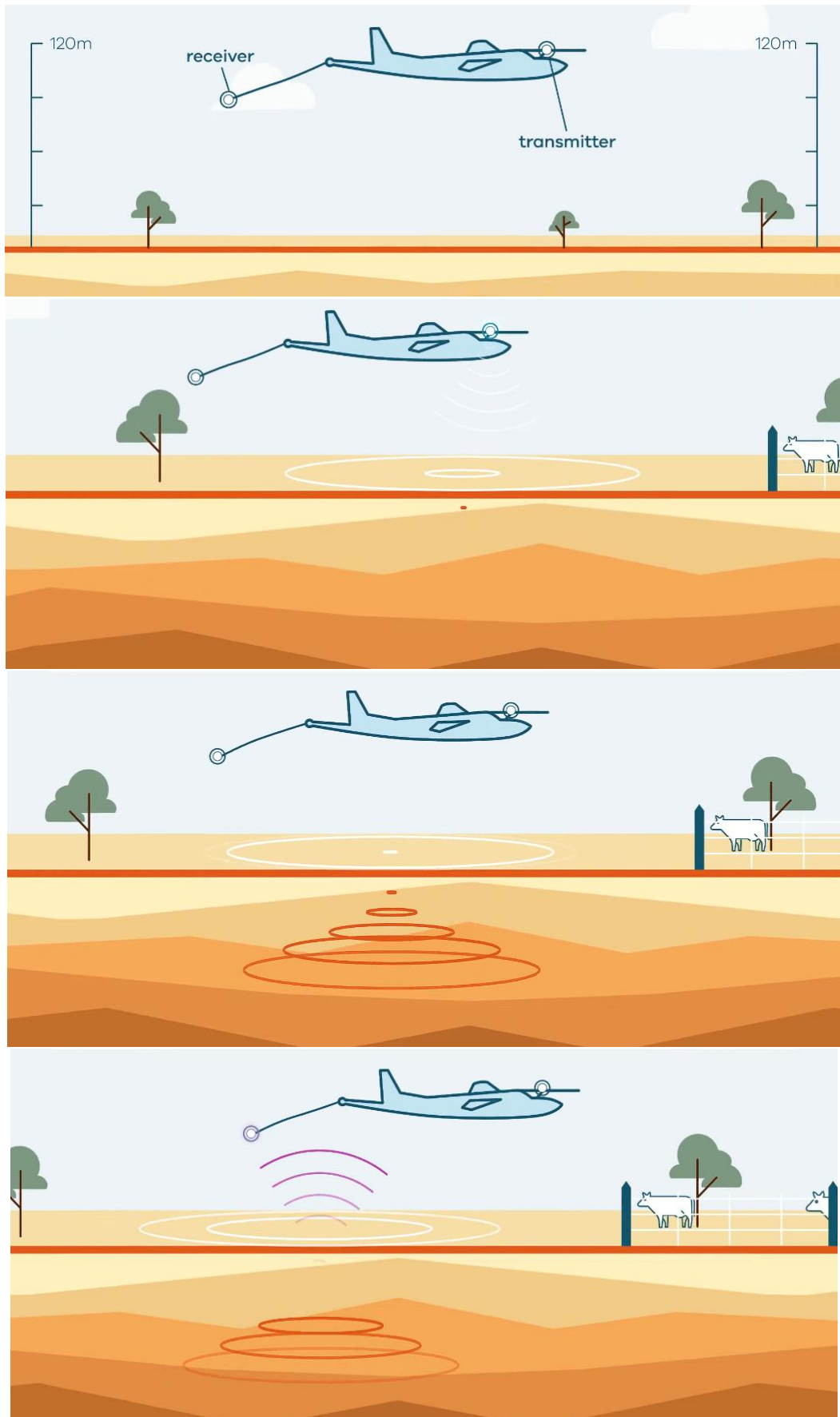


Figure 5.2 - AEM System working scheme

AEM surveys offer significant advantages due to their ability to cover large areas quickly and provide high-resolution conductivity information. The method is non-invasive, making it suitable for environmentally sensitive areas. However, its effectiveness depends on the conductivity contrasts present in the subsurface and can be influenced by factors such as noise, system design, and survey conditions.

The versatility of AEM surveys makes them an essential tool in mineral exploration, groundwater management, and environmental assessment. By combining advanced acquisition techniques with rigorous data processing and interpretation, AEM provides a powerful means of visualizing subsurface conductivity variations, enabling informed decision-making in resource exploration and land-use planning. The following section outlines the survey technique applied in the Paterson AEM survey, along with the considerations and processing methods used to interpret the AEM data and generate the final inversion models.

The Paterson survey was flown with FAS' TEMPEST™ AEM system which was installed on the CASA C-212-200 aircraft (Figure 5.3) registered VH-TEM on the Australian civil aircraft register (Table 5.1).



Figure 5.3 - CASA C-212-200 aircraft photo

Table 5.1 Aircraft information

Manufacturer	CASA
Model	C212-200 Turbo Prop
Registration	VH-TEM
Ownership	Fugro Airborne Surveys Pty Ltd

The TEMPEST™ system is a state-of-the-art airborne time-domain electromagnetic system specifically designed for high-precision mapping of subsurface geological structures (Table 5.2). Its operation is based on detecting the electromagnetic (EM) response generated by the interaction of a primary electromagnetic field, produced by a transmitter loop, with subsurface layers. This technology is widely used for mineral exploration, including uranium deposits, particularly those associated with paleovalleys.

The core principle of TEMPEST™ lies in generating a series of electromagnetic pulses transmitted through a single-turn transmitter loop mounted around the nose, wings, and tail of the aircraft. These pulses induce eddy currents in conductive subsurface layers, which, in turn, generate a secondary electromagnetic field recorded by the receiver coils. Materials with high conductivity cause slower decay of secondary currents, whereas low-conductivity materials result in more rapid decay, enabling characterization of subsurface layers.

The transmitter loop is mounted on an aircraft flying approximately 122 meters above the ground. The base signal frequency is adjustable, and pulse durations can be tailored from 0.6 to 4 milliseconds, allowing the system to adapt to different geological targets. The receiver coils, housed in a towed sensor capsule, are positioned 35 meters below and 120 meters behind the aircraft. This design minimizes noise and ensures precise data acquisition.

The receiver system comprises three orthogonal coils that measure the rate of change of the magnetic field (dB/dt). However, only the X- and Z-components are used for data processing, providing sufficient detail for interpretation. The exact geometry of the transmitter and receiver setup is critical, as it directly impacts the measurement results. GPS systems, radar and laser altimeters, and gyroscopes, which monitor aircraft roll, pitch, and yaw, are employed to maintain geometric accuracy.

Data processing involves separating the total recorded response into the primary field (direct transmitter-receiver interaction) and the secondary field (caused by eddy currents in the subsurface layers). This information is then used to build subsurface conductivity models that reflect geological structures.

TEMPEST™ is distinguished by its high precision, flexible configurations, and efficiency in complex geological and climatic conditions. The system enables detailed mapping of material conductivity and analysis of geological features over large areas. Its application enhances exploration efficiency, reduces costs, and provides critical data for subsequent geological and economic evaluations of deposits.

Of particular significance is the role of TEMPEST™ in paleovalley exploration, where large uranium deposits are often located. The system enables in-depth interpretation of the structure and composition of these geological formations, making it an indispensable tool for the modern phase of mineral exploration. These estimated geometry parameters are then used in standard inversion algorithms to derive subsurface conductivity models from the measured data.

Electromagnetic Receiver and Data Logging Computer. The electromagnetic (EM) receiver primarily utilized the Picodas PDAS-1000 data acquisition system. However, during the final survey flight (Flight 114), the EMFASDAS system replaced

the Picodas. Both receiver systems operated proprietary software designed to manage system control, timing, data acquisition, and storage. A synchronization card coordinated timing, triggering, and precise alignment between the TEMPEST transmitter and digital signal processing (DSP) modules. This synchronization relied on the Pulse Per Second (PPS) signal from the integrated GPS module. Additionally, the synchronization feature ensured precise magnetic data acquisition in relation to the transmitter's signal.

During system calibration and survey line data collection, the receiver computer displayed critical performance metrics on its primary screen, enabling the operator to monitor data quality and system functionality in real-time.

**TEMPEST Transmitter.** The transmitter produced an alternating polarity square wave, triggered directly by the EM receiver system. The nominal operating frequency was set at 25 Hz, with a pulse width of 10 ms (50% duty cycle). A current transformer within the circuit monitored the waveform, logging both its shape and amplitude. The data were sampled and recorded by the EM receiver for detailed analysis.

**TEMPEST Three-Axis Towed Bird Assembly.** The TEMPEST three-axis towed bird assembly accurately captured low-noise data for the X (inline horizontal), Y (transverse horizontal), and Z (vertical) electromagnetic field components. Due to reduced sampling rates, Y-component data were excluded from the delivered dataset. The assembly's receiver coils measured the rate of change of the magnetic field (dB/dt), transmitting signals via a specialized cable designed for both electrical conductivity and mechanical durability.

**Survey Computers: PDAS 1000 and FASDAS.** Both survey computers ran proprietary software to gather and log positional, magnetic, and auxiliary data. Information was displayed in real-time in numerical and graphical formats on a VGA LCD display. The operator could adjust sensitivity during the survey to facilitate quality control.

**Cesium Magnetometer Sensor.** The airborne system included a cesium vapor magnetometer consisting of a sensor head, a cable, and electronic modules. The sensor was mounted on a composite material boom extending from the aircraft's tail.

**Magnetometer Processor Board.** Processor boards from Picodas and FASDAS were used to handle the Larmor frequency output from the magnetometer sensor. These boards interfaced with the survey computer to initiate and time data collection while ensuring synchronization with the EM receiver system.

**Fluxgate Magnetometer.** A three-axis Bartington MAG-03MC fluxgate magnetometer was installed on the tail boom to measure the aircraft's attitude, which was used to correct the total magnetic field measurements.

**GPS Receiver.** Positioning and navigation were facilitated by a Novatel GPSCard 951R, which logged satellite range data for post-survey differential corrections.

**Differential GPS Demodulator.** Real-time differential corrections were provided by the OMNISTAR service to enhance positioning accuracy.

Table 5.2 - TEMPEST™ AEM System Specifications

Attribute	Specification
Base frequency	25 Hz
Transmitter area	221 m <sup>2</sup> (VH-TEM)
Transmitter turns	1
Waveform	Square
Duty cycle	50%
Transmitter pulse width	10 ms
Transmitter off time	10 ms
Peak current	280 A (VH-TEM)
Peak moment	61,880 Am <sup>2</sup> (VH-TEM)
Average moment	30,940 Am <sup>2</sup> (VH-TEM)
Sample rate	75 kHz on X and Z components
Sample interval	13.333 microseconds
Samples per half cycle	1,500
System bandwidth	25 Hz to 37.5 kHz
TX loop flying height nominal	121.1 m (subject to safety)
TX loop flying height average	122.4 m (VH-TEM)
EM sensor	Towed bird with 3-component dB/dt coils
TX-RX horizontal separation average	120.1 m (VH-TEM)
TX-RX vertical separation average	34.5 m (VH-TEM)
TX-RX horizontal separation standard	120 m (geometry-corrected)
TX-RX vertical separation standard	35 m (geometry-corrected)
Stacked data output interval	200 ms (~12 m spatial)
Number of output windows	15
Window centre times	13 $\mu$ s to 16.2 ms
Magnetometer	Stinger-mounted caesium vapour
Magnetometer compensation	Fully digital
Magnetometer output interval	200 ms (~12 m spatial)
Magnetometer resolution	0.001 nT
Typical noise level	0.2 nT
GPS cycle rate	1 second

Navigation System. Navigation during the survey was managed by Picodas PNAV 2001 and, in Flight 114, by FASDAS navigation computers. These systems loaded pre-programmed flight plans, including boundary coordinates, line endpoints, and other survey parameters, transforming GPS data into local coordinates for precise cross-track and distance-to-go calculations. Data were displayed graphically and numerically to assist pilots in maintaining the intended flight path.

#### Altimeter System

1) Radar Altimeter: The Sperry Stars RT-220 radar altimeter had a sampling interval of 0.2 seconds and accuracy of  $\pm 1.5\%$  of the indicated altitude.

2) Laser Altimeter: The Optech 501SB laser altimeter offered precision of  $\pm 0.05$  m at survey altitudes with a similar sampling interval.

3) Barometric Altimeter: Altitude was calculated using data from a Digiquartz 215A-101 pressure transducer, which measured atmospheric pressure via a probe mounted on the aircraft wingtip.

Video Tracking System. A digital video recording system synchronized video files with geophysical data using digital fiducial markers. The files included GPS coordinates and survey line identifiers.

Airborne Data Logging. The PDAS Survey computer records all other survey data including aeromagnetic and GPS data as "S" Survey files, and "R" Rover files containing GPS raw range data for post processing. The FASDAS Survey computer records a continuous MSD file which contains all other ancillary data including magnetic, altimeter, GPS and analog channels.

## 5 Paterson Orogen - gravity and aeromagnetic interpretation

### 5.1 Gravity Characteristics

The Rudall Complex is distinguished by pronounced Bouguer gravity anomalies ranging from approximately  $-350$  to  $-50 \mu\text{m}\cdot\text{sec}^{-2}$ , which correspond closely with known outcropping areas (see Figure 3.2). A prominent zone of elevated gravity values, about 150 km wide, extends from the Southwest Thrust–McKay Fault Zone in the south to the northern sector of the Paterson North region. This zone is bounded on the west by the Vines Fault, a major structural boundary, while to the east gravity values decrease markedly over a zone approximately 30 km wide. This eastern gradient is attributed to the increasing thickness of sedimentary rocks in the adjacent Canning Basin, where the basement exhibits significantly different Bouguer anomaly signatures—typically ranging from  $-350$  to  $-450 \mu\text{m}\cdot\text{sec}^{-2}$ .

Red corresponds with high, and blue low, Bouguer anomaly. Anomalies typical of granite greenstone terrane of the Pilbara Craton extend eastward under the Fortescue and Hamersley Basins to the Vines Fault. Rudall Complex in outcrop and underlying the Yeneena Basin is thought to be responsible for the 150 km wide zone of general north-northwest-trending gravity high to the east of the Vines Fault. Local gravity lows in this zone are attributed to: overlying Coolbro Sandstone, between the Southwest Thrust and Mount Eva Fault; Paleozoic sediments in the Waukarlycarly Embayment, central Paterson north; and, in some instances, intruded granite. Major faults are inferred to disrupt the Rudall Complex and influence the distribution of overlying sediments

The zone of high gravity anomalies is interpreted as representing the continuation of the Rudall Complex beneath the younger sedimentary cover of the Yeneena Basin. The crustal characteristics of the Rudall Complex differ substantially from those of the adjacent East Pilbara granite-greenstone terrane. In particular, the Rudall Complex exhibits higher average Bouguer gravity values and lacks the localized, moderate amplitude gravity lows (on the order of tens of  $\mu\text{m}\cdot\text{sec}^{-2}$ ) that are associated with large, approximately 30 km diameter granite massifs typical of the East Pilbara terrane. This suggests notable differences in rock composition, density, and possibly crustal thickness between these adjacent geological provinces.

Structurally, the Rudall Complex is dissected by major fault zones. Among them, the Coolbro Fault plays a key role. This significant fault cuts through the southern part of Paterson North and is inferred to act as a boundary separating distinct geological formations, specifically the Broadhurst and Isdell formations.

The Coolbro Fault is interpreted as a long-lived, active tectonic feature that has influenced not only structural but also sedimentary evolution across the region. Its continued activity during various orogenic events points to its importance in regional crustal deformation.

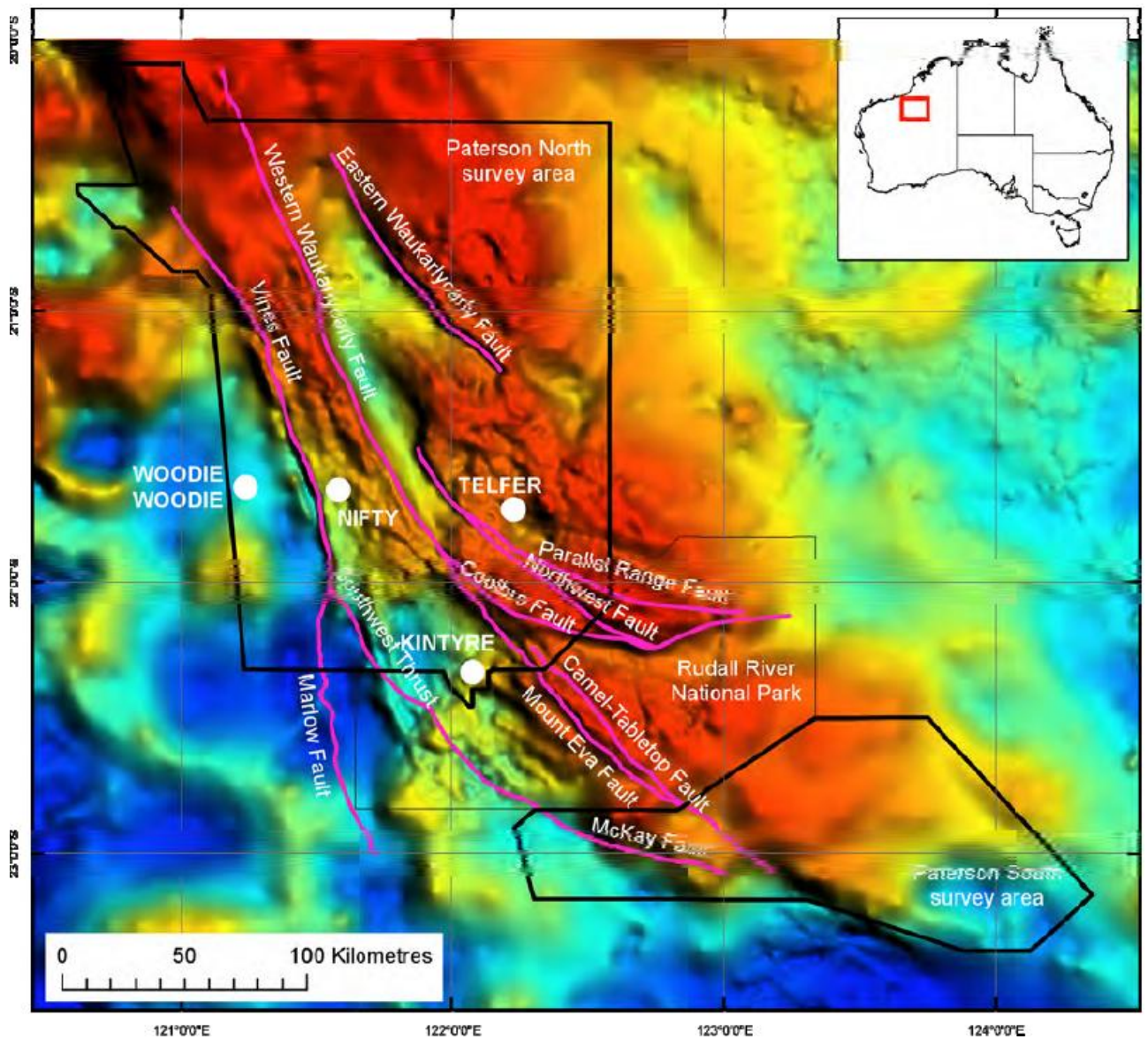


Figure 5.1 - Gradient-enhanced Bouguer anomaly gravity with a 500 m grid cell size

On the western margin of the Rudall Complex, the zone between the Vines Fault and the Waukarlycarly Embayment shows a dense network of linear features trending north-northwest. This pattern of faulting indicates more intense deformation compared to the eastern margin, suggesting a complex tectonic history with multiple phases of crustal reactivation. This western area also coincides with a transition into the Pilbara Craton and its overlying sedimentary basins, which have been mapped with relatively coarse spatial resolution (11 km station spacing), limiting the precision of structural and density models in this area (Figure 5.1).

In the northeastern sector of Paterson North, the Lamil Group underlies much of the terrain either at surface exposures or shallow depths. This group is associated with broad gravity highs roughly 20 km across, exhibiting Bouguer anomaly values 50 to 100  $\mu\text{m}\cdot\text{sec}^{-2}$  higher than the Rudall Complex outcrops to the south. Conversely, the overlying Coolbro Sandstone in the southwestern portion of Paterson North correlates

with notable gravity lows, approximately 200–300  $\mu\text{m}\cdot\text{sec}^{-2}$  lower than the Rudall Complex. This difference reflects the significantly lower density of sandstone compared to the predominantly mafic and intermediate rocks of the Rudall Complex. The Lamil Group's higher carbonate content relative to the Throssell Range Group suggests a higher average density for the former, consistent with the higher amplitude gravity anomalies observed.

Gravity gradients detected on the southern approaches to the Coolbro Fault are interpreted as reflecting thickening of the Throssell Range Group sediments near the fault zone. Additionally, localized gravity lows coincide with granitic intrusions identified through aeromagnetic surveys, highlighting the complex lithological variations and structural overprints influencing the gravity field. These combined factors—rock density contrasts, sediment accumulation, and fault-related disruption—create a complex geophysical signature requiring integrated data interpretation.

## 5.2 Aeromagnetic Characteristics

Aeromagnetic data provide further insights into the Rudall Complex's structural and lithological framework (Figure 3.3). The complex is divided into two primary parts, west and east, separated by a broad, northwest-trending structural zone linked to the Camel Tabletop–Mount Eva Fault system. The western segment, encompassing the Talbot and Connaughton terranes, is characterized by low to moderate magnetic intensities. These areas are dominated by mafic to intermediate volcanic and intrusive rocks with relatively subdued magnetic signatures.

In contrast, the eastern Tabletop Terrane exhibits stronger and more complex magnetisation patterns, with large, irregularly shaped granite bodies that display higher magnetic susceptibility. Additionally, this region contains several small, highly magnetised intrusive bodies of uncertain composition. These features suggest a more diverse intrusive history and possible magmatic differentiation compared to the western terranes.

The sedimentary cover of the Yeneena Basin mostly shows weak magnetic responses, reflecting the dominance of non-magnetic sedimentary rocks. However, certain units within the Broadhurst and Wilki formations demonstrate moderate magnetic intensities, offering valuable markers for regional structural interpretation and basin architecture.

The Coolbro Fault is a prominent feature in both gravity and magnetic datasets, confirming its status as a key tectonic boundary within the Rudall Complex. Its clear geophysical signature underlines its importance as a locus of strain localization and as a boundary separating different lithological and structural domains.

During the orogenic events known as the Miles and Paterson orogenies, the Camel Tabletop–Mount Eva Fault likely experienced reactivation, involving both vertical displacement and strike-slip movements. This fault system serves as a major

tectonic boundary that partitions the Rudall Complex into distinct terranes and controls the spatial distribution of lithologies and structural fabrics observed today.

#### Regional Geophysical Integration and Interpretation

The integration of gravity and aeromagnetic data provides a comprehensive picture of crustal composition, structure, and tectonic boundaries across the Rudall Complex and its surroundings. Gravity surveys, despite their relatively coarse spatial resolution (station spacing between 2.5 and 11 km), reveal major crustal density variations and fault zones but have limitations in resolving finer near-surface structures. Aeromagnetic data, with higher spatial resolution and sensitivity to variations in magnetic mineralogy, complement gravity data by delineating near-surface lithological boundaries and intrusive bodies. However, the generally weak magnetisation of many rock units within the region limits the interpretative detail in some areas.

These combined geophysical datasets confirm the presence and significance of key tectonic boundaries such as the Coolbro Fault and the Camel Tabletop–Mount Eva Fault system. These structures have played critical roles in the tectonic evolution of the Rudall Complex, acting as zones of crustal weakness, facilitating deformation, and influencing sedimentary basin development.

The complex interplay between lithology, structural deformation, and sedimentation evidenced by these geophysical observations underscores the heterogeneity of the crust in this part of the Paterson region. These insights are crucial for guiding mineral exploration, understanding crustal growth and modification processes, and reconstructing the tectonic history of the region where direct geological observations are often obscured by thick sedimentary cover.

White corresponds with high-magnetisation and black with low-magnetisation. Highly magnetised banded iron formation in greenstone of the Pilbara Craton extends under the Fortescue Group to the west of the Vines Fault. In the Rudall Complex, Paterson South and southern-most Paterson North, folded compositional layering in the Talbot and Connaughton terranes southwest of the Camel-Tabletop Fault contrasts with textures attributed to abundant granite in the Tabletop Terrane to the northeast and east. (Figure 5.2.1)

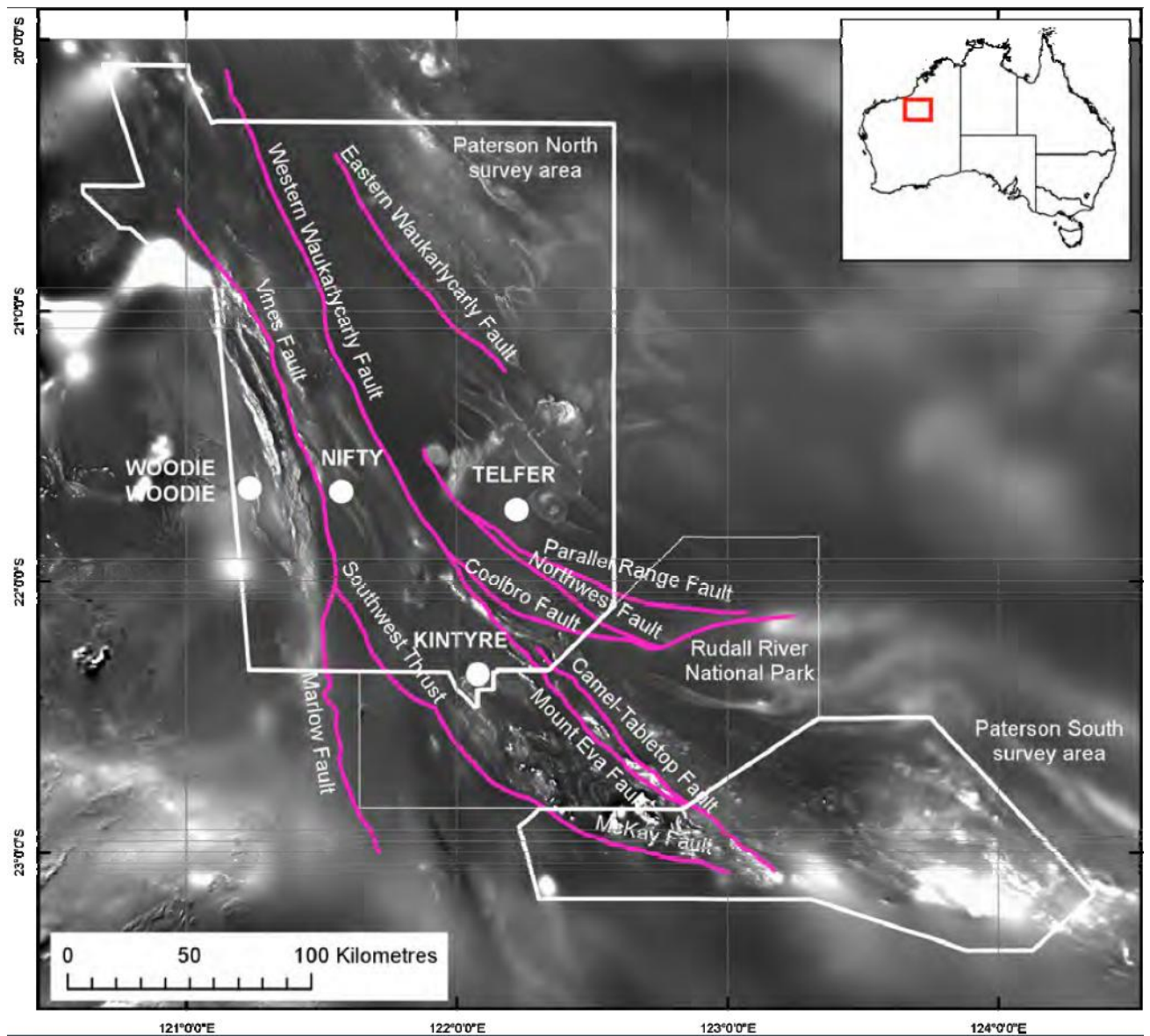


Figure 5.2.1 - Image of total magnetic intensity data with an 80 m grid cell size.

Structural trends and complexity of the Rudall Complex in Paterson South and southern-most Paterson North contrast with simpler bedding trends of the Lamil Group in northeast Paterson North. Granite of the Mount Crofton and O'Callaghans suites cut dominantly northwest bedding trends and faults in the Lamil Group. Fault-disrupted gentle folds in the Tarcunyah Group are seen to the south of the McKay Fault. (Figure 5.2.2)

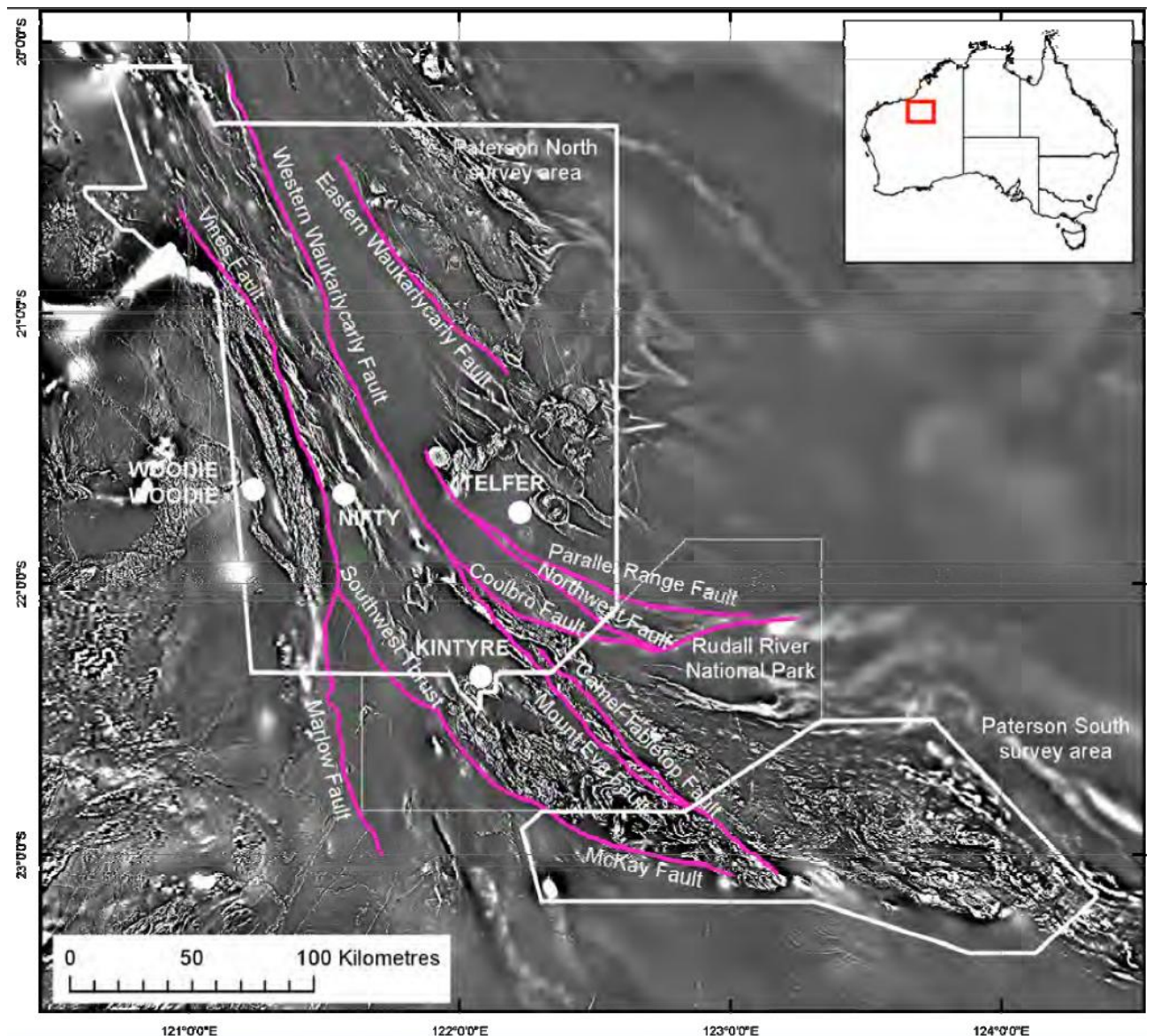


Figure 5.2.2 - Image of the first vertical derivative of total magnetic intensity with an 80 m grid cell size

### 5.3 Canning Basin

The onshore Canning Basin spans over 430,000 km<sup>2</sup>, encompassing the Great Sandy and Gibson deserts. Its geological history began in the Early Ordovician and was largely completed by the Early Cretaceous. The Paterson area is located on the northwest margin of the Canning Basin, where it overlaps the Archean Pilbara Craton, the Paleoproterozoic Rudall Complex, and the Neoproterozoic Yeneena Basin.

In the Paterson area, Permian and Mesozoic sedimentary rocks are exposed, while older rocks are interpreted based on seismic sections within the Waukarlyarly Embayment. This section summarizes data on the distribution, lithology, and thickness

of these rocks, which will be used for the geological interpretation of AEM data and the assessment of uranium mineral systems in the area.

**Permian Deposits.** In the Paterson area, the identified Permian sequences include fluvio-glacial deposits of the Paterson Formation and shallow marine facies of the Poole Sandstone, Noonkanbah Formation, and Triwhite Sandstone. These strata are grouped into distinct stratigraphic units.

**Paterson Formation:** Comprises a basal layer of poorly sorted, unstratified mudstone with abundant dropstones and thinly bedded quartz wacke. The upper layers consist of cross-bedded fluvial sandstones and conglomerates containing pebbles and boulders of Precambrian origin. Thickness ranges from 33 m at the type section to over 400 m within the Canning Basin. This formation is associated with a fluvio-glacial environment.

**Poole Sandstone:** Characterized by interbedded thin sandstone and mudstone layers with ripple marks, indicating deposition in a shallow marine environment. Thickness at the type section is approximately 33 m.

**Noonkanbah Formation:** Dominated by fine calcareous mudstones and a rich marine fauna, suggesting a quiet, standing water environment. Pyritic zones indicate reducing conditions. Thickness varies from 6 m to 290 m.

**Triwhite Sandstone:** Confined to areas near Sahara and Tabletop, with exposures up to 8 m thick, though it reaches 77 m in the WAPET Kidson 1 well. The upward coarsening of grain size indicates a shallow-water regressive marine environment.

**Mesozoic Deposits.** In the Paterson area, Mesozoic sedimentary sequences are primarily distributed north and northeast of the Percival Palaeovalley system, west of Lake Winifred, and east of the Disappointment Palaeovalley system. The total thickness of Mesozoic units in this region is estimated at less than 100–200 meters.

**Alexander Formation (Late Jurassic):** Comprising sandstone interbedded with mudstone (20–92 m thick), this unit represents a shallow marine to tidal facies and occurs predominantly on Joanna Spring.

**Bardwine Sandstone (Late Jurassic):** A fluvial facies, found outside the primary survey area.

**Cronin Sandstone (Late Jurassic to Early Cretaceous):** Confined to the Runton area, this sandstone is correlated with the Callawa Formation. It includes fine- to coarse-grained sandstone, minor mudstone, and conglomerates.

**Callawa Formation (Late Jurassic to Early Cretaceous):** Found in the northeast, this fluvial facies consists of poorly sorted sandstone and conglomerate (52–80 m thick).

**Parda Formation (Early Cretaceous):** Thin-bedded to massive mudstone and fine sandstone, this unit (up to 30 m thick) suggests a lagoonal or shallow marine environment.

**Frezier Sandstone (Early Cretaceous):** Sandstone and minor conglomerate (approximately 15 m thick), interpreted as a basinward facies of the Callawa Formation.

**Anketell Sandstone (Early Cretaceous):** This shallow marine sandstone (less than 50 m thick) overlies other formations disconformably. It is likely that Mesozoic

sediments were more laterally continuous before being incised and reworked by the Wallal, Percival, and Disappointment palaeovalley systems, which also eroded underlying Permian sediments.

**Cenozoic Deposits.** The Oakover Formation is the primary Cenozoic bedrock unit in the Paterson area. It consists of lacustrine carbonates up to 50 m thick, with a lower carbonate-rich unit and an upper chalcidonic unit. This formation occupies much of the Oakover River valley. Other Cenozoic materials, classified as regolith, include unconsolidated sediments and soils.

**Tectonics and Deformation.** In the northern Paterson Range, well-bedded sandstones are intensely deformed, forming disharmonic folds and fault zones interpreted as results of glacial movement or sediment instability due to melting ice. Seismic data reveal faults in the Paterson Formation sediments within the Waukarlycarly Embayment, likely associated with growth faults along the basin boundary.

**Mineralogical Features.** The Paterson Formation is notable for glacially-derived dropstones of various Precambrian rock types, some with faceted and striated surfaces. In glaciolacustrine facies, these dropstones are embedded in massive mudstone matrices, often displaying Liesegang banding. In fluvioglacial facies, the dropstones occur throughout the sequence alongside fluvial conglomerate lenses.

AEM and aeromagnetic surveys have identified major fault systems and sediment thickness variations. For instance, in the Waukarlycarly Embayment, growth faults influence sediment accumulation. These datasets provide insights for localizing potential uranium mineralization zones.

**Research Prospects.** The Canning Basin, particularly the Permian and Mesozoic deposits in the Paterson area, offers a unique setting for studying sedimentary processes associated with glacial and fluvioglacial conditions. Data on lithology, thickness, and tectonic features provide a foundation for further investigations of uranium mineralization and other geological processes. The integration of mineralogical studies with AEM and other methods enhances understanding of the basin's evolution and resource potential.

## **5.4 Kintyre deposit**

**Discovery and Historical Context of the Kintyre Deposit.** The Kintyre deposit was discovered in April 1985 by CRA Exploration Pty. Ltd. (now Rio Tinto Exploration Pty. Ltd.) following detailed airborne radiometric surveys conducted by helicopter. Radiometric anomalies were key to identifying uranium mineralization exposed at the surface. Drilling began in October the same year, with the first hole intersecting a 77-meter zone averaging 0.25%  $U_3O_8$ , indicating significant industrial potential.

By 1988, resources were estimated at 36,000 tons of  $U_3O_8$  with grades from 0.15% to 0.40%, making Kintyre the largest hydrothermal uranium deposit and the second largest uranium mine in Western Australia. Kintyre is central to a system of

uranium occurrences within the Paleoproterozoic and Mesoproterozoic Rudall Complex. Other notable deposits in the region include Tracy (Yandagooge), Lead Hills to the north, and Wellington and smaller deposits to the south.

Although publicly available information on Kintyre is limited, key geological and mineralization studies have been published by Jackson & Andrew (1990), Gauci & Cunningham (1992), Hickman & Clarke (1993), and McKay & Mieizitis (2001).

#### Geological Features and Deposit Structure

Kintyre lies within the Rudall Complex, where ore bodies are hosted by metasediments of the Yandagooge Formation. Wellington and nearby deposits occur in quartzites with iron ore bands. Most uranium deposits are concentrated along major northwest–southeast trending shear zones.

Structurally, Kintyre consists of five main ore zones: Kintyre-East, Kintyre, Whale, East Whale, Pioneer, and Nerada. Uranium mineralization is predominantly pitchblende located in narrow carbonate-chlorite veins dipping about 60° northeast, aligned with regional shear faults.

Host rocks include chlorite-quartz and chlorite-carbonate-quartz schists and garnet-bearing quartzites, overlain by dolomites and underlain by biotite-graphite schists. Multiple folding stages have localized ore veins in fold hinges parallel to axial planes. Faults and thrusts oriented parallel to folds segment ore bodies into lenses.

**Mineralogy and Age of Uranium Mineralization.** Mineralogy is diverse, with colloform pitchblende as the main uranium mineral in veins. Other minerals include bismuthinite, chalcopyrite, bornite, galena, plus traces of gold and platinum group elements. The geochemical association of gold with copper and bismuth reflects complex hydrothermal processes.

Ore zones exhibit intense chloritization of host rocks and complete garnet alteration to chlorite, along with carbonate replacements and magnetite-to-martite transformation. Pitchblende also occurs microscopically in wallrocks at lower concentrations.

TIMS dating places the deposit age at about  $841 \pm 10$  million years (Late Proterozoic), currently the best constraint on the timing of uranium vein formation in the Rudall Complex.

**Geophysical Characteristics and Exploration Methods.** Geophysical studies included ground and airborne magnetic, radiometric, electromagnetic surveys, gravity, electrical resistivity, and induced polarization (IP) measurements. The key discovery feature was a radiometric anomaly in bismuth-214—a decay product of uranium-238—with a 300–400 m width and uranium concentrations up to 8 ppm.

Regional geophysical anomalies are present but only radiometric anomaly correlates clearly with uranium mineralization. Magnetic data show low-amplitude, short-wavelength maxima; gravity surveys detected local density highs related mainly to dense metapelitic rocks rather than ore bodies.

Resistivity data indicate the presence of current-resistant host rocks such as metachert, carbonates, and quartzites. IP surveys revealed strong responses spatially coincident with mineralization, reflecting both sulfides and the presence of pitchblende and graphite.

Additional conductivity data suggest possible deep conductive zones associated with regional faults and graphite schists, warranting further investigation.

### Conclusions and Significance for Integrated Uranium Deposit Forecasting

Kintyre exemplifies classic hydrothermal uranium mineralization in structurally complex carbonate-chlorite veins formed by multi-stage folding and tectonic processes. Geological, mineralogical, and geophysical data provide a comprehensive understanding of ore formation and distribution, crucial for exploration and research.

Studying Kintyre supports development of integrated geophysical-geological methods to improve predictive accuracy for uranium prospects. Combining radiometric data with geophysical techniques such as magnetic and IP surveys enhances detection of concealed ore bodies and insight into regional geodynamics.

This experience can be applied in similar uranium-bearing regions, including Kazakhstan and neighboring countries, to advance mineral exploration strategies.

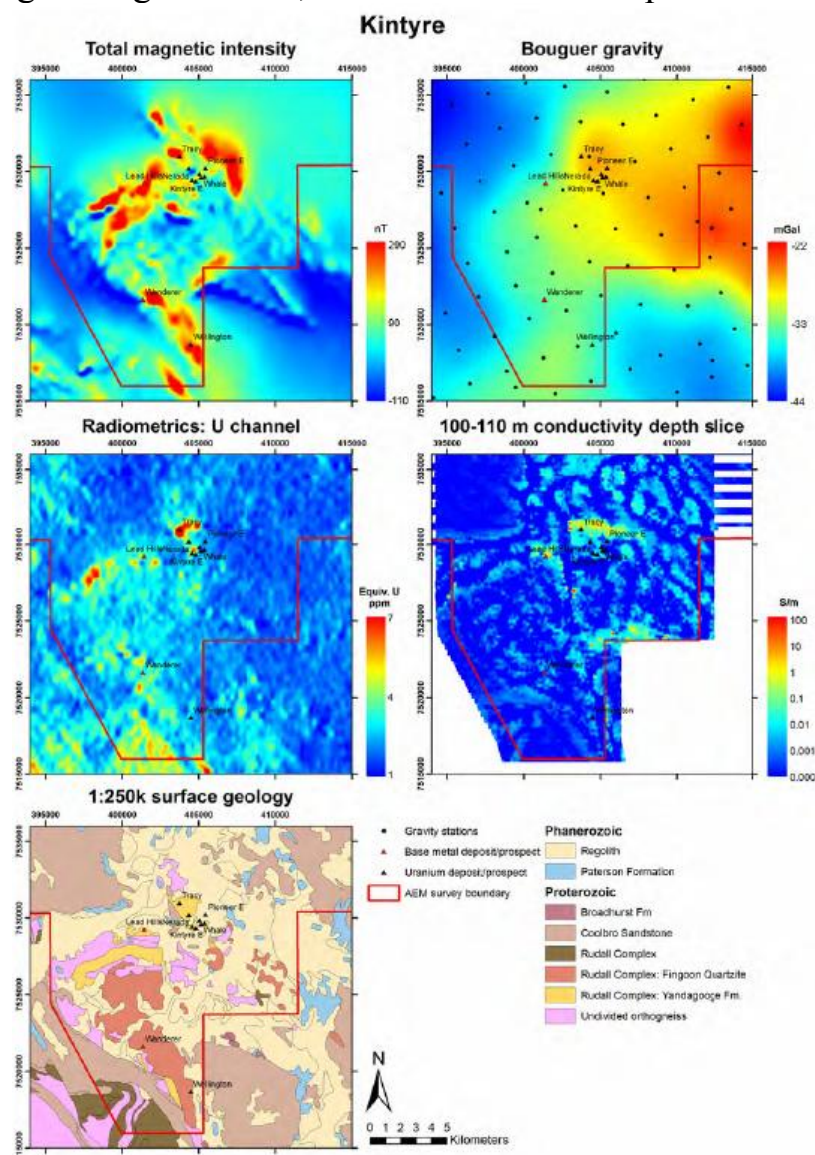


Figure 5.4.2 - Geophysical signature of the area surrounding the Kintyre uranium deposit. Total magnetic intensity, Bouguer gravity and radiometric data are extracted from the Geophysical Archive Data. Delivery System (GADDs: <http://www.ga.gov.au/gadds>)

## **6 Comparative analysis of Australia and Kazakhstan**

Australia and Kazakhstan hold leading positions in the global uranium industry, boasting significant reserves and well-developed extraction infrastructure. Australia is renowned for its advanced geophysical exploration technologies, while Kazakhstan extensively utilizes the In-Situ Leaching (ISL) method for uranium extraction. Adapting Australian geophysical methods to Kazakhstan's conditions presents a significant opportunity to enhance the efficiency and economic viability of uranium exploration.

Australia employs comprehensive geophysical methods for uranium deposit exploration. Among the most effective technologies is airborne gamma-ray spectrometry, used to identify radioactive anomalies. This technique allows for rapid and precise identification of zones with elevated concentrations of radioactive elements such as uranium, thorium, and potassium. Magnetic and gravimetric surveys are actively employed to determine the structural features of ore bodies, simplifying the modeling of their spatial distribution. Electromagnetic methods and induced polarization (IP) also play a crucial role in detailing structures and assessing their conductivity. These approaches have led to the discovery of large deposits such as Olympic Dam and Ranger and facilitated the development of three-dimensional geological models. As a result, prediction accuracy has significantly improved, and drilling risks have decreased.

Kazakhstan possesses the world's largest uranium reserves, predominantly found in sandstone formations. These geological features make ISL the most applicable and economically efficient extraction method in the country. However, the geophysical methods currently employed in Kazakhstan, such as electrical prospecting and downhole gamma-ray spectrometry, primarily focus on maintaining ongoing extraction processes and monitoring activities. The potential for modernization and expanded use of advanced approaches remains substantial. Implementing Australian technologies in Kazakhstan could substantially improve the accuracy of uranium deposit exploration. Integrating airborne gamma-ray spectrometry and magnetic surveys would enable more precise localization of uranium anomalies, especially crucial for deeply buried ore bodies. The use of three-dimensional geological models could reduce the number of ineffective drill holes and lower costs. Additionally, machine learning techniques could be adopted to analyze geophysical data and evaluate the filtration properties of rocks, optimizing the leaching process and enhancing uranium recovery rates.

The economic feasibility of introducing Australian technologies in Kazakhstan is justified by long-term benefits. Initial investments associated with personnel training, equipment acquisition, and technology adaptation would be offset by reduced exploration time, lower drilling costs, and increased recoverable reserves. Accurate exploration methods would also decrease the likelihood of unnecessary environmental disruptions, aligning with contemporary sustainability requirements. Furthermore, improved monitoring of ISL processes could minimize ecological risks and ensure the long-term safety of extraction operations.

Particular attention should be given to leveraging Australia's experience in automation and digitalization. In Australia, unmanned technologies for airborne geophysical surveys and data processing are actively developed. Integrating such technologies in Kazakhstan could significantly enhance the productivity of exploration activities and facilitate real-time decision-making based on data analysis. The successful implementation of projects such as Olympic Dam could be adapted to the development of Kazakhstan's major deposits, considering local geological and climatic conditions.

Kazakhstan, with its advanced position in the uranium industry, already demonstrates successful adoption of innovative methods. For instance, the joint venture with the Canadian company Cameco at the Inkai deposit exemplifies the effective application of ISL and a comprehensive approach to monitoring technological parameters. However, the adoption of more precise exploration methods could further improve efficiency and competitiveness.

The application of Australian geophysical exploration technologies in Kazakhstan represents a promising avenue for enhancing the uranium sector's efficiency. Integrating advanced approaches such as airborne gamma-ray spectrometry, three-dimensional modeling, and process automation could yield significant economic and environmental benefits. These advancements would enable Kazakhstan to strengthen its position in the global uranium market while maintaining sustainable industry development. This exchange of expertise between the two countries underscores the importance of international collaboration in addressing global energy challenges.

## CONCLUSION

The system of paleovalley uranium deposits in Australia and Kazakhstan includes four key components that are interrelated and facilitate deposit formation processes:

- 1) sources of ore-forming elements (leachable uranium, vanadium, and potassium) associated with paleovalleys, which supply the necessary minerals;
- 2) paleovalleys and basin margins, serving as migration pathways and accumulation zones for these elements;
- 3) physicochemical conditions for mineralization, such as paleogeomorphology, groundwater flow and salinity, pH, Eh, and climatic conditions creating a favorable environment for uranium ore formation; and
- 4) preservation conditions for deposits before and after mineralization (clay covers, tectonic disturbances, and erosion processes).

Paleovalley uranium deposits in Australia and Kazakhstan are located in the marginal parts of sedimentary basins and their peripheral paleovalleys, ranging in age from the Carboniferous to the Cenozoic. These deposits are widespread in the western, southern, and northern parts of Australia, as well as in Kazakhstan.

Given the proximity of known uranium sources, there is significant potential for discovering new deposits in these regions. For example, in Kazakhstan, the Chu-Sarysu and Syrdarya basins have high potential for forming paleovalley deposits. Here, paleovalley systems are associated with uranium-bearing sedimentary rocks of Mesozoic-Cenozoic age, making these regions active targets for geological exploration.

For Kazakhstan, the most promising areas are the Chu-Sarysu and Syrdarya basins, where paleovalley systems are connected to uranium-bearing sedimentary rocks of Mesozoic-Cenozoic age. Horizontal lithological-geochemical mapping of the Cretaceous and Paleogene in the Chu-Sarysu uranium province has made it possible to create a three-dimensional geological and hydrogeological model, including 1:200,000 scale maps of seven Paleogene and Upper Cretaceous horizons, as well as a structural map and a pre-Mesozoic surface map. This model can serve as a basis for further exploration of mineral resources in the sedimentary cover and the upper part of the pre-Mesozoic complex.

Paleovalley uranium models play an important role in exploration, as they allow the integration of a wide range of geological factors contributing to deposit formation. Improved understanding of geological conditions and landscape history helps refine exploration targets and select appropriate methods for paleovalley mapping. Regional studies of paleovalley uranium deposits can be based on empirical data obtained from known deposits. Models evolve as new data are accumulated through geological exploration and sedimentological studies.

The exploration process begins with a preliminary analysis of paleodrainage systems using cost-effective methods such as remote sensing and comparative data analysis in GIS. The next stage involves refining the model using geophysical methods,

including airborne geophysical surveys and drilling. The final stage includes the creation of three-dimensional geological models, which enable the mapping of sedimentary facies, tracking of lithological changes, identification of structural features, and detailed assessment of mineralization systems.

Organogenic sands, clays, calcite, and lignites of Mesozoic and Cenozoic age are the main hosts of uranium deposits in the paleovalleys of Kazakhstan. These regions remain promising for the discovery of new deposits. Similar geological conditions of uranium-bearing basins in Kazakhstan emphasize the need for prioritizing these territories for further research and enhancing exploration efficiency.

The analysis of geological conditions in Australia and Kazakhstan shows that paleovalley systems and arid climates are key factors in the formation of uranium deposits. These conditions facilitated uranium migration and the creation of large deposits, which hold strategic significance for the mining industry. By integrating advanced exploration methods and technologies, such as airborne electromagnetic (AEM) surveys, with geological modeling, exploration efficiency and success rates can be significantly improved.

A strategic focus on the Chu-Sarysu and Syrdarya basins will likely yield substantial benefits for Kazakhstan's uranium industry, fostering the discovery of new deposits and contributing to the advancement of the nation's mining sector.

## REFERENCES

- 1 Geological and energy implications of the Paterson Province airborne electromagnetic (AEM) survey, Western Australia. GEOSCIENCE AUSTRALIA RECORD 2010/12 By I. C. Roach (editor). With contributions from: K. F. Cassidy, M. T. Costelloe, K. Czarnota, P. Duerden, D. K. Hutchinson, D. Huston, S. Jaireth, S. F. Liu, D. Maidment, D. Miggins, I. C. Roach, C. Sorensen, A. J. Whitaker, J. R. Wilford and N. C. Williams.
- 2 Petrov N.N., Tsalyuk Y.I., Khasanov E.G., Malakhov A.A. et al. Report on deep geological mapping of the Mesozoic-Cenozoic cover of the Chu-Sarysu Depression on a scale of 1:200000 sheets L-42-XXII, XXXII(124), XXXIII,XXXIV, K-42-III(5-B; 6-A,B,G),IV(7,8) for 1996-2001 in 3 books.
- 3 M. Lawrence, L. Stenning: Paterson North Airborne Electromagnetic (AEM) Mapping Survey.
- 4 Aden D. McKay & Yanis Mieztis. AUSTRALIA'S URANIUM RESOURCES, GEOLOGY AND DEVELOPMENT OF DEPOSITS.
- 5 Baohong Hou , John Keeling, Ziyang Li.:Paleovalley-related uranium deposits in Australia and China: A review of geological and exploration models and methods.
- 6 Hickman, A.H., & Clarke, G.L. (1994). Geology of the Broadhurst 1:100,000 Sheet. Western Australia Geological Survey, 1:100,000 Geological Series Explanatory Notes.
- 7 Curtis, J.L., Brunt, D.A., Binks, P.J., 1990. Tertiary palaeochannel uranium deposits of South Australia. In: Hughes, F.E. (Ed.), Geology of the mineral deposits of Australia and Papua New Guinea. Australasian Institute of Mining and Metallurgy, pp. 1631–1636. Monograph 14.
- 8 Curnamona Energy, 2009. Annual Report 2009. Curnamona Energy Ltd.
- 9 Dahlkamp, F.J., 1993. Uranium Ore Deposits. Springer-Verlag, Berlin Heidelberg.
- 10 Dahlkamp, F.J., 2009. Uranium Deposits of the World. Springer Ed., Asia. 493 pp.
- 11 Dai, J., 1996. Metallogenic geological conditions of the Russian paleovalley uranium deposits. Uranium Geol. 12 (6), 336–340 (in Chinese with English abstract).
- 12 de Broekert, P.P., 2002. Origin of Tertiary inset-valleys and their fills, Kalgoorlie, Western Australia Unpublished Ph.D. thesis. Australian National University, Canberra, Australia. 388 p.
- 13 DeVoto, R.H., 1978a. Uranium geology and exploration: lecture notes and references. Colorado School Mines, Golden. 396p.
- 14 DeVoto, R.H., 1978b. Uranium in Phanerozoic sandstone and volcanic rocks. In: Kimberley, M.M. (Ed.), Uranium deposits, their mineralogy and origin, 3. Mineralogical Association of Canada, pp. 293–306. Short Course Handbook.

- 15 Dickson, B.L., 1984. Uranium series disequilibrium in the carnotite deposits of Western Australia. Surficial Uranium Deposits TECDOC-322. IAEA, Vienna, pp. 165-170.
- 16 Acclaim, 1999. Acclaim Uranium NL Annual Report 1999.
- 17 Andrew, R. L., 1988. Kintyre uranium deposit and the Rudall Province. Uranium Institute Symposium, London, September 1988.
- 18 ANRA, 2009. Australian Natural Resources Atlas. Online: <http://www.anra.gov.au/>.
- 19 ASRIS, 2009. Australian Soil Resource Information System. Online: <http://www.asris.csiro.au/>.
- 20 Bagas, L., 2000. Geology of the Paterson 1:100 000 sheet - Explanatory Notes. Geological Survey of Western Australia, Perth. 20 p.
- 21 Bagas, L., Williams, I. R. and Hickman, A. H., 2000. Rudall, Western Australia (2nd Edition). 1:250 000 Geological Series - Explanatory Notes. Western Australia Geological Survey. 50 p.
- 22 Bautin, F. and Hallenstein, C., 1997. Plans for uranium mining by COGEMA. In: ANA 97 Conference on Nuclear Science and Engineering in Australia, 1997. Australian Nuclear Association Inc., Sydney. 20-24 pp.
- 23 Beard, J. S., 1990. Plant life of Western Australia. Kangaroo Press, Kenthurst NSW.
- 24 BOM, 2009. Bureau of Meteorology. Online: <http://www.bom.gov.au/>.
- 25 Brunt, D. A., 1990. Miscellaneous uranium deposits in Western Australia. In: Hughes, F. E. (ed) Geology of the Mineral Deposits of Australia and New Guinea. Australasian Institute of Mining and Metallurgy, Melbourne. 1615-1620 pp.
- 26 Cameron, E., 1990. Yeelirrie Uranium Deposit. In: Hughes, F. E. (ed) Geology of the Mineral Deposits of Australia and New Guinea. Australasian Institute of Mining and Metallurgy, Melbourne. 1625-1629 pp.
- 27 Brodie, R., and Fisher, A., 2008, Inversion of TEMPEST AEM survey data, Honeysuckle Creek, Victoria: Geoscience Australia for the Bureau of Rural Sciences.
- 28 Brodie, R., and Sambridge, M., 2009, Holistic inversion of frequency-domain airborne electromagnetic data with minimal prior information: Exploration Geophysics, 40, 765-78.
- 29 Ray, A., Symington, N., Ley-Cooper, Y., Brodie, R.C. 2020. A quantitative Bayesian approach for selecting a deterministic inversion model. Geoscience Australia, Canberra.